

A Stereotaxic Template Atlas of the Macaque Brain for Digital Imaging and Quantitative Neuroanatomy

RICHARD F. MARTIN AND DOUGLAS M. BOWDEN

*Regional Primate Research Center and Department of Psychiatry and Behavioral Sciences,
University of Washington, Seattle, Washington 98195*

Received March 29, 1996

A stereotaxic brain atlas of the longtailed macaque (*Macaca fascicularis*) is presented in a format suitable for use as a template atlas of the macaque brain. It includes most of the brain segmented to show the boundaries of landmark structures such that every point in the brain can be represented by a unique set of coordinates in three-dimensional space and ascribed unambiguously to one and only one primary structure. More than 400 structures are represented, including 360 volumetric structures, which constitute the substance of the brain, and 50 superficial features. To facilitate use with ventriculography, magnetic resonance imaging, and other noninvasive imaging techniques, the stereotaxic space is referenced to internal landmarks, viz., the anterior commissure and posterior commissure; the center of the anterior commissure at the midline is the origin of the stereotaxic axes. Reference of stereotaxis to this bicommissural space facilitates structural comparison with human brain atlases, which are commonly referenced to the bicommissural line. It also facilitates comparison of brains of different nonhuman primate species by providing a template brain against which to compare size and internal variability. Thirty-three coronal sections at 1-mm intervals from the spinomedullary junction to the rostral extreme of the caudate nucleus show most structures of the hindbrain, midbrain, and subcortical forebrain. Separately, four side views and 16 coronal sections show cortical structures. Structures are represented by outlines of their boundaries and labeled according to NeuroNames, a systematic English nomenclature of human and nonhuman primate neuroanatomy. Abbreviations are based on a protocol designed to facilitate cross-species comparisons. Instructions are provided for: (1) locating sites from the Template Atlas in the conventional stereotaxic space of an experimental animal, (2) locating sites identified by conventional stereotaxis in the Template Atlas, and (3) using the Template Atlas to collate, compare, and display image information (e.g., labeled cells, recording sites, stimulation sites, lesions) from multiple animals. © 1996 Academic Press, Inc.

INTRODUCTION

Neuroanatomical information derived from imaging and histological labeling techniques can make its full contribution to understanding brain function only if one can relate it to knowledge gained by other techniques. The most direct way of linking image information from diverse sources is through mapping onto a standard template brain segmented according to classical neuroanatomy (Bowden and Martin, 1996). For more than 20 years the explosive growth in knowledge of the neurochemistry of the rat brain has been facilitated by comprehensive, detailed atlases onto which the distributions of diverse neuronal characteristics and functions have been mapped and compared (Koenig and Klippel, 1963; Paxinos and Watson, 1986; Pellegrino and Cushman, 1967; Swanson, 1992).

Ungerstedt (1971) was among the first to summarize the location of neuromarkers on a template brain. Using Koenig and Klippel's (1963) stereotaxic atlas of the rat brain, he mapped information from a number of studies about the monoamine pathways. This allowed other investigators to test hypotheses about the role of the monoamine pathways in brain function. For example, in a review of intracranial self-stimulation in the rat, we were able to transcribe more than 800 sites from 17 different studies onto the Ungerstedt maps. Quantitative comparisons indicated significant overlap of self-stimulation sites with three of the catecholamine pathways (German and Bowden, 1974).

There has long been a need for a similar atlas of the macaque brain. While macaques represent the genus of nonhuman primate most commonly studied in U.S. neuroscience (Bowden, 1989; D. M. Bowden and R. F. Martin, unpublished data, 1992), a comprehensive template brain atlas suitable for summarizing image information from diverse sources has not been available. Several features would be desirable in such an atlas. (1) It should be stereotaxic, so that every point in the brain can be identified with a unique set of coordinates in a three-dimensional space that is readily related to the coordinate systems of modern imaging

technology. (2) The brain should be segmented such that structures are represented by contours of their boundaries so that the landmarks for identifying homologous locations are as unambiguous as possible. (3) It should be comprehensive, i.e., it should include as much of the brain as possible, and every point in the brain should be represented in one and only one landmark structure. (4) It should be as detailed as possible, so that all landmarks identifiable in conventionally stained sections are represented. (5) Structures should be named and labeled according to a nomenclature that reflects as clearly as possible known homologies with the human brain and other mammalian species.

These features, while not available from any one source, are represented to one extent or another in the various textbooks and atlases of human and nonhuman primate neuroanatomy which we have consulted during development of this atlas of the macaque brain. Stereotaxic atlases of the macaque brain, while generally not indicating the boundaries of structures, show locations of most subcortical structures and some cortical landmarks. The most comprehensive of the conventional macaque atlases are based on several different species. These include the rhesus macaque (*Macaca mulatta*) (Snider and Lee, 1961), the longtailed macaque (*M. fascicularis*) (Shantha *et al.*, 1968; Szabo and Cowan, 1984), the pigtailed macaque (*M. nemestrina*) (Winters *et al.*, 1969), and the Japanese macaque (*M. fuscata*) (Kusama and Masako, 1970). Since the subcortical structure of other nonhuman primates differs very little from that of the macaque, one should add to this list the excellent comprehensive atlases of the squirrel monkey (*Saimiri sciureus*) (Emmers and Akert, 1963) and the common marmoset (*Callithrix jacchus*) (Stephan *et al.*, 1980).

The number of structures labeled in the conventional atlases ranges from 110, in an atlas based on photographs of unstained frozen sections to minimize stereotaxic distortion (Szabo and Cowan, 1984), to 318, in an atlas based on processed sections stained for Nissl substance and myelin to maximize structural detail (Shantha *et al.*, 1968). One can obtain greater detail for some brain areas from regional atlases devoted to specific parts of the macaque brain, such as the cortex (Bonin and Bailey, 1947; Krieg, 1975), olfactory areas (Turner *et al.*, 1978), thalamus (Benevento, 1975; Olszewski, 1952), hypothalamus (Bleier, 1984), basal forebrain (Mesulam *et al.*, 1983), midbrain (Benevento, 1975), brain stem (Smith *et al.*, 1972), amygdala (Amaral *et al.*, 1992), and locus ceruleus and its projections (Bowden *et al.*, 1978; German and Bowden, 1975).

For many computerized applications every point in a region of interest must be located in a structure and all structures must be mutually exclusive. This is essential for filing and retrieving information from multiple

brains, comparing brains from experimental and control groups, and merging data sets from multiple laboratories. Ambiguity of classification can lead to erroneous retrieval. A comprehensive and mutually exclusive set of neuroanatomical structures is also necessary for quantitative analysis of image information on the distribution of variables such as neurochemical markers, cellular density, stimulation sites, and drug injection sites. Without comprehensiveness and mutual exclusivity of structural categories one cannot calculate numbers or densities of items in a superstructure based on their distribution in its substructures. Unambiguous representation of structures requires that their boundaries be specified.

Oertel's (1969) atlas of the rhesus macaque brain provides boundaries and meets the criteria of comprehensiveness of segmentation and mutual exclusivity of structures. It is limited, however, to the brain stem, it is not stereotaxic, and the planes of section are so different from the coronal plane of the standard stereotaxic atlases as to impede accurate transfer of data from standard coronal sections to the template sections.

Szabo and Cowan's (1984) atlas of the *M. fascicularis* brain comes closest to meeting the need for a template atlas. It is stereotaxically based, includes most of the brain, and provides the most detailed segmentation of any atlas to date. With only about one-third of the most salient structures labeled, however, large areas remain unsegmented and unnamed, so the locations of many of the classical landmark structures that neuroanatomists use to describe and map new neuromarkers are not indicated. In many respects, the present atlas can be viewed as an extension of the Szabo and Cowan atlas to include a more comprehensive and detailed segmentation of structures and to provide a stereotaxic coordinate system more suited to applications involving ventriculography, magnetic resonance imaging (MRI), and other modern imaging techniques.

MATERIALS AND METHODS

Subjects and Brain Preparation

The Template Atlas is based on tracings of coronal sections from the brains of two representative young adult male longtailed macaques (*M. fascicularis*; also known as crab-eating macaque, Java monkey, cynomolgus monkey, and *M. irus*). Monkey 1 weighed 3.6 kg; monkey 2 weighed 3.4 kg. The study was conducted in accord with procedures currently approved by the Animal Care Committee of the University of Washington.

Each animal was anesthetized with ketamine and chloralose to the surgical level of anesthesia and placed in a stereotaxic instrument (Kopf, Tujunga, CA). The instrument was fitted with elevated earbars to allow acquisition of a lateral ventriculogram unobstructed by the side bars of the instrument. Ventriculography was

performed with metrizamide (Amipaque; Winthrop Laboratories, New York). Following procedures reported in an earlier study of six longtailed macaques in which we assessed the range of variability between cranial landmarks and internal landmarks of this species (Dubach *et al.*, 1985), a lateral X-ray ventriculogram was filmed to show the anterior commissure (ac), posterior commissure (pc), and other internal landmark structures (Fig. 1). The bicommissural line was plotted by connecting the centers of ac and pc on the ventriculogram. The orientation of the cranium in the stereotaxic instrument was adjusted by raising or lowering the eyebars to make the bicommissural line parallel to the horizontal plane of the stereotaxic apparatus. This adjustment aligned the brain in the "bicommissural space," a rectangular coordinate system in which the bicommissural line is parallel to the anteroposterior (AP) axis of the stereotaxic instrument. By means of Kopf electrode carriers, vertical stainless steel rods were placed through the brains perpendicular to the bicommissural line 10 mm to the right and left of the midline and 15 mm rostral to the intermeatal (ear bar) line. The rods were left in place throughout the period of freezing or fixation, leaving a pair of lines that clearly established the coronal plane of bicommissural space. All tissue sections were taken parallel to this plane.

Immediately after surgery the animal was euthanized by intracardiac perfusion (1 liter buffered Ringer's solution, for both animals, followed by 4 liters 10% buffered formalin for monkey 2, whose brain was destined for histology). To minimize distortion of the relation between forebrain and brain stem during fixation, both animals were perfused while in the sitting position with the cranium in the stereotaxic instrument (Smith *et al.*, 1972). To minimize distortion of the brain relative to the cranium during perfusion, the neck was ligated before the perfusion pressure was reduced and remained ligated while the cranium was removed. The cranium was then frozen (monkey 1) or immersed for fixation (monkey 2; 10% formalin for 35 days, 30% sucrose/10% formalin for 10 days).

The brain of monkey 1 was dissected frozen in a cold room and suspended stereotaxically in a sucrose solution which was frozen to produce a cylindrical block suitable for mounting on a specially constructed sliding microtome. It was cut by microtome with a camera mounted such that the face of the block could be photographed before each section was taken. The sections were cut at 40- μ m thickness, which resulted in approximately 1200 photographs. The specimen obtained with this procedure had a minimum of distortion and was used primarily to provide information on cortical landmarks.

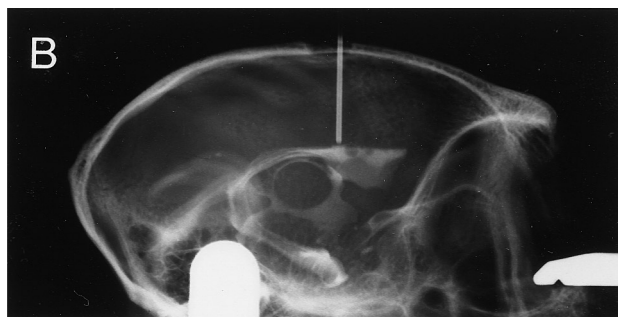
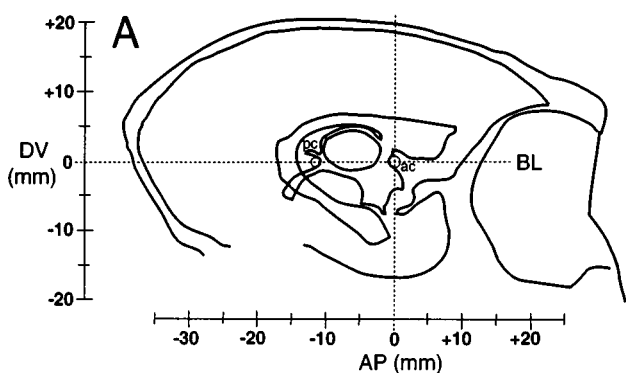


FIG. 1. Landmarks that define the bicommissural space. (A) The vertical plane is defined by the midline sagittal section of the brain. The horizontal plane is perpendicular to the vertical plane through the bicommissural line (BL), which is, in turn, defined by the centers of the anterior commissure (ac) and posterior commissure (pc). These structures are readily visible by (B) ventriculography and by (C) magnetic resonance imaging. The origin of the bicommissural space is the center of ac. AP, anteroposterior axis; DV, dorsoventral axis.

The brain of monkey 2 was removed from the cranium, measured, and embedded in egg yolk to maintain the relation between portions of sections that might become dissociated during cutting and mounting. The yolk-embedded brain was exposed to fumes from a 30% formalin solution for 12 days until the tissue/yolk block was thoroughly cured (Simmons, 1979). A single block extending from caudal occipital cortex to the rostral boundary of the caudate nucleus was cut in serial 40- μ m sections on a freezing microtome. Every fifth section was stained for Nissl substance (cresyl violet) and the adjacent section was stained for myelin (Weil). This procedure yielded a complete set of coronal sections at 200- μ m intervals from the spinomedullary junction to the rostral extreme of the caudate nucleus.

Stereotaxic Coordinate System

For most of the 20th century the horizontal reference plane for stereotaxis in nonhuman primates has been the orbitomeatal plane, i.e., the plane defined by the inferior orbital ridges and the external auditory meati. Some atlases define the horizontal zero plane as the orbitomeatal plane itself (Frankfurt plane); others define it as parallel to the orbitomeatal plane but 10 mm dorsal to it (Horsley-Clarke plane). The locations of intracerebral structures relative to the cranial landmarks are notoriously unreliable, particularly in the longtailed macaque which has a highly variable cranial structure (Percheron and Lacourry, 1973). In this species the distance from the inner surface of the calvarium, and thus the top of the brain, to the orbitomeatal plane can vary over a range of almost 5 mm (Dubach *et al.*, 1985). Indeed, there is a systematic difference of about 4 mm in the dorsoventral coordinates of homologous structures in the two existing atlases of the *M. fascicularis* brain (Shantha *et al.*, 1968; Szabo and Cowan, 1984).

The widespread use of ventriculography (Dubach *et al.*, 1985; Feger *et al.*, 1975; Ilinsky and Kultas-Ilinsky, 1982; Percheron, 1975) and MRI (Alvarez-Royo *et al.*, 1991; Rebert *et al.*, 1991; Saunders *et al.*, 1990) in primate stereotaxic procedures has partially liberated neuroscientists from dependence on cranial landmarks as reference points in brain stereotaxis. Internal landmarks are much better than conventional cranial landmarks for accurate guidance of electrodes and cannulas, or for locating areas of neuronal activity imaged by MRI, PET, or other means. To take advantage of the stereotaxic accuracy made possible by noninvasive imaging of intracerebral landmarks, the coordinate system of the Template Atlas (Fig. 1) is referenced to the bicommissural line and interhemispheric plane, landmarks which have become standard in human brain imaging and neurosurgery (Downs *et al.*, 1994; Mazziotta *et al.*, 1995; Schaltenbrand and Wahren,

1977; Schieman *et al.*, 1994; Talairach *et al.*, 1957; Talairach and Tournoux, 1988).

While the concept of bicommissural space has become standard in human brain stereotaxis, the operational definition of ac and pc and the origin of the axes of the space have not. Different authors at different times have specified these differently (Downs *et al.*, 1994). In the Template Atlas ac and pc are defined as the centers of the structures as best estimated from a ventriculogram or a midline sagittal MRI. The origin of the bicommissural space, i.e., the point where the coordinates of the AP, dorsoventral (DV), and mediolateral (ML) axes are all 0, is the center of ac (Fig. 1).

Nomenclature

To facilitate comparisons between the macaque brain and human brain, structures are named according to a standard English nomenclature which includes terms from both human and nonhuman primate neuroanatomy. It is based on NeuroNames, a computer-based, structured system of classical neuroanatomical terminology which contains most of the English and Latin synonyms applied to structures of the human and nonhuman primate brain (Bowden and Martin, 1995, 1996; Martin *et al.*, 1990). NeuroNames is a HyperCard application for Macintosh desktop computers, which includes more than 5000 terms.¹ By clicks of the mouse on a succession of "cards," the user navigates through a semantic network to identify the relationships of terms to one another and to the hierarchy of structures which constitute the primate brain.

The core of the semantic network is the NeuroNames Brain Hierarchy (Bowden and Martin, 1995). The Hierarchy provides a description of the primate brain in terms of an exhaustive set of mutually exclusive substructures at each level. It is based on the hierarchy inherent in the *Nomina Anatomica* (IANC, 1983) and elaborated according to a number of standard English-language textbooks of neuroanatomy, particularly *Human Neuroanatomy* (Carpenter and Sutin, 1983), *Correlative Anatomy of the Nervous System* (Crosby *et al.*, 1962), *An Atlas of the Basal Ganglia, Brain Stem and Spinal Cord* (Riley, 1943), *The Human Nervous System* (Paxinos, 1990), and *Neuroanatomy and the Neurologic Exam* (Anthoney, 1994).

In the NeuroNames Hierarchy, "BRAIN" at the highest level is subdivided through nine levels of "superstructures" down to a comprehensive set of 501 nonoverlapping "primary structures." The goal in the development of this atlas was to represent as many of the primary

¹The NeuroNames database was copyrighted in 1991 by the University of Washington. Incorporation of the NeuroNames Brain Hierarchy into a computerized knowledge base for commercial distribution requires establishment of a derivative works agreement with the University of Washington.

structures as could be identified in conventionally stained histologic sections of the macaque brain. The NeuroNames Hierarchy also contains 165 "superficial structures" which do not contribute to brain volume, but which belong to specific volumetric subdivisions of the brain. Included in the superficial structures, for example, are the cortical sulci and the cranial nerves. The Template Atlas illustrates as many of these superficial structures as we could identify.

NeuroNames was released by the Primate Information Center in 1990 as a HyperCard application on diskette. The English nomenclature of NeuroNames has been incorporated into the Digital Anatomist Browser,² a computer application developed by the Department of Biological Structure at the University of Washington to teach basic human neuroanatomy to medical students (Brinkley *et al.*, 1993), and the Metathesaurus of the National Library of Medicine's Unified Medical Language System (Tuttle *et al.*, 1990). It has been used as a standard against which to compare other neuroanatomical nomenclatures developed for special purposes, such as the Index for Radiological Diagnoses of the American College of Radiology and the Systematized Nomenclature of Medicine (Sato *et al.*, 1993). In 1995 the hierarchy was revised to make it more consistent with human neuroanatomic textbooks and compendia currently in widest use in graduate departments of anatomy in the United States (Bowden and Martin, 1995).

Abbreviations

To facilitate comparisons between the Template Atlas and other sources, the abbreviations used to label structures are based on a system designed to represent English terminology and to facilitate recognition of homologous structures in the brains of primates, rodents, and other mammalian species (Paxinos and Watson, 1986). This is an important feature, because much of our tentative knowledge about the human brain is based on the 70% of brain research conducted on the rodent brain (Bowden, 1989). To the extent justified by neuroanatomical determination, use of the same names and labels for homologous structures will improve understanding of the brain. The abbreviations of terms for homologous structures are taken from the rat atlas of Paxinos and Watson (1986) or constructed on the basis of conventions adopted in that work (Bowden and Martin, 1995). With a few exceptions, such as abbreviations for the thalamic nuclei for which long-established abbreviations are widely used as primary names, abbreviations in NeuroNames and the Template Atlas follow the word order of English termi-

nology. Abbreviations which begin with capital letters represent nuclei; fiber tracts are represented by lowercase letters. Compound names of nuclei have a capital letter for each word or meaningful subunit. If more than the first letter of a word is required to create a unique abbreviation, the letter of second greatest mnemonic value (not necessarily the second letter of the term) is provided in lowercase. Arabic numerals are used to identify cranial nerves.

Segmentation and Drawing of Structures

Drawings of the structures in coronal sections were made by tracing boundaries with a mouse and cursor on a live video image of the Nissl-stained histological section. The tracing system consisted of a Macintosh-fx computer (Apple, Cupertino, CA) with a ColorSpace II/FX graphics board (Mass Microsystems, Sunnyvale, CA) and Adobe Illustrator software (Adobe, Seattle, WA). Ambiguities in the live video images were resolved by reference to a complete set of paper and pencil tracings of images (7× magnification) produced from the same sections by overhead projector (Bausch & Lomb, Rochester, NY) using a 2.7× objective lens. Ambiguities in the projected images were resolved as far as possible by light microscopic examination of the sections at 25× and 40× magnification. Every effort was made to resolve boundaries to within 200 μm.

The computerized drawing program, Adobe Illustrator, allows one to record different features of an image in separate "layers" which are subsequently superimposed to provide a composite, finished illustration. The boundaries of all structures were traced into the first or "template boundary" layer such that the cross-section of each structure was represented by a continuous line in a closed contour. The contours of adjacent structures were superimposed so that they appear as one in the image, but each structure can be treated as an independent object by the Illustrator software.

To produce the coronal illustrations in the Template Atlas (Figs. 3 and 4) five other layers of the image were created in registration to the first layer. A "label layer" contained the abbreviations of structure names. An "indicator layer" contained the lines which connect labels (abbreviations) to their structures. A "shading layer" contained the gray-level shading of gray structures and ventricles. A "clarity layer" contained dotted and solid lines to indicate the relative clarity of portions of boundaries in the first layer, and a "scale layer" contained the stereotaxic scale which surrounds the image.

Storing different features of an image in separate layers allows one to generate images in a number of formats by merging different combinations of layers. Depending on the need, one can crop, enlarge, or reduce the scale and eliminate any class of detail (labels, dotted lines, shading, stereotaxic scale) which would

² The URL of the Digital Anatomist Browser on the World Wide Web is <http://www1.biostr.washington.edu/DigitalAnatomist.html>.

mask the data that a user wants to apply to the template boundary layer.

RESULTS AND DISCUSSION

Images of 33 coronal Nissl-stained sections taken at 1.0-mm intervals through the hindbrain, midbrain, and subcortical forebrain of the second animal were traced and segmented to produce the drawings of cortex presented in Fig. 3 and the drawings of subcortical structures presented in Fig. 4. From these sections we were able to reconstruct and segment all of the major subdivisions of the brain represented in the NeuroNames Hierarchy except for the olfactory bulb, the hypophysis, the cerebellar cortex and the frontal and occipital poles of the cerebral cortex. A complete representation of the sulcal and gyral patterns of the cerebral cortex (Fig. 2) was produced by combining dorsal, ventral, medial, and lateral projections from the coronal sections of this brain with a set of drawings similar to that of the first animal. Thus, while the surface drawings of the cortex are complete, they represent a merger of image information from two brains and do not match stereotaxically the coronal sections of cortex in Fig. 2.

We were able to identify and label a total of 410 structures listed in NeuroNames as basic components of the primate brain. Of the total, 360 were volumetric structures, i.e., structures that combine to constitute the substance of the brain, and 50 were superficial structures, e.g., sulci and appendages. The NeuroNames Brain Hierarchy (Bowden and Martin, 1995) includes a total of 501 primary structures, i.e., the basic set of volumetric structures that combine to form the hierarchical superstructures of the brain. Primary NeuroNames structures that we failed to identify included: (1) structures of the human cortex that are not found in the macaque, e.g., the transverse temporal gyri and subdivisions of the inferior frontal gyrus and insula; (2) layered cellular structures that were too thin to represent at the level of resolution of the atlas, e.g., the seven layers of superior colliculus and five layers of the inferior colliculus; (3) subdivisions of white matter structures that have no clear histologic boundaries and that are not evident in coronal section, such as the five subdivisions of the internal capsule; (4) subdivisions of cellular structures in which boundaries in our material were unclear and/or the labeling was so variable in the atlases we reviewed that identification was ambiguous, e.g., four subdivisions of the basolateral nuclear group of the amygdaloid nuclear complex, five subdivisions of the solitary nucleus, and several nuclei of the pretectal region and superior olivary complex; (5) primary structures that are not readily distinguishable in conventionally stained material, e.g., nucleus subceruleus; and (6) nerve tracts that are so diffusely distributed through

nuclear areas that they do not reach the criterion of 50% white matter necessary to be identified separately from the nuclei in which they are embedded, e.g., the olivocerebellar tract and the reticulospinal tract.

Comparability of the Template Atlas to Other Atlases of the *M. fascicularis* Brain

The brain used to generate the coronal sections of the Template Atlas was obtained from an animal selected as representative of six long-tailed macaques previously studied for range of variability in internal landmarks (Dubach *et al.*, 1985). Grossly it was also representative of the animals on which previous atlases of this species were based (Table 1). The weight, length, and width of the template brain were very near the means reported for animals in the 3.0 to 4.0-kg weight range used in the *M. fascicularis* brain atlases of Szabo and Cowan (1984) and Shantha *et al.* (1968).

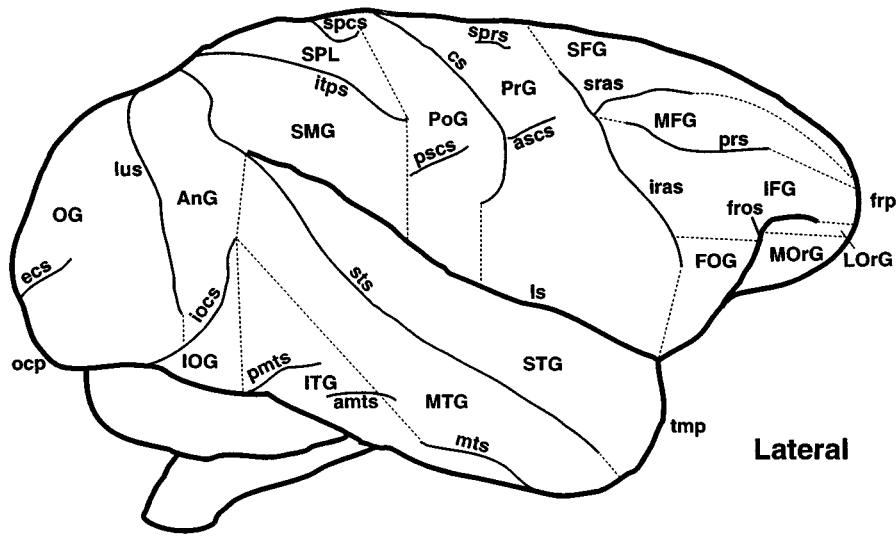
To assess further the degree to which the internal structure of the template brain was representative of the *M. fascicularis* species we translated a number of landmarks in the Szabo and Cowan (1984) atlas of the *M. fascicularis* brain into the bicommissural coordinate system of the Template Atlas and compared their locations. This was done by translating the orbitomeatal coordinate system of the conventional atlas into the bicommissural coordinate system (Taylor, 1959) and determining the variability in location of its structures relative to those of the template brain.

The landmarks selected for comparison of the two atlases (Table 2) were all points that appeared in both atlases and that could be specified with relatively high precision (± 0.5 mm in the AP dimension; ± 0.2 mm in the DV and ML dimensions). They were also selected to represent an even distribution through the full extent of the cortical and subcortical regions included in Fig. 4, i.e., anteroposteriorly from the spinomedullary junction to the junction of the temporal and frontal lobes (AP -23 to AP $+5$), dorsoventrally at a wide range of levels (DV -18 to DV $+19$), and laterally from the midline to the body and tail of the caudate nucleus (ML 0 to ML $+12$). Most of the landmarks were centers of

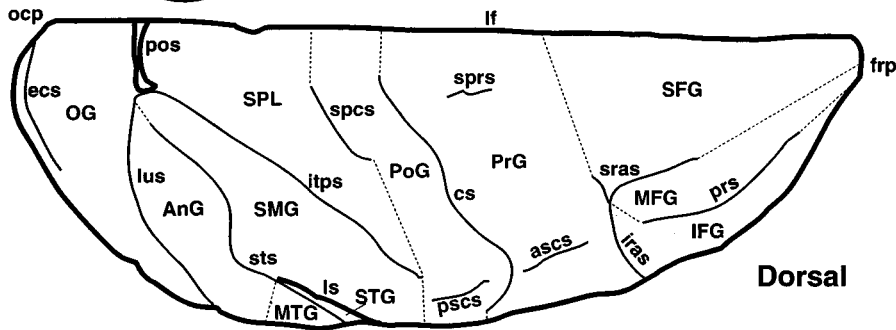
TABLE 1

Comparison of Template Brain with the Brains on Which Other *Macaca fascicularis* Atlases Are Based

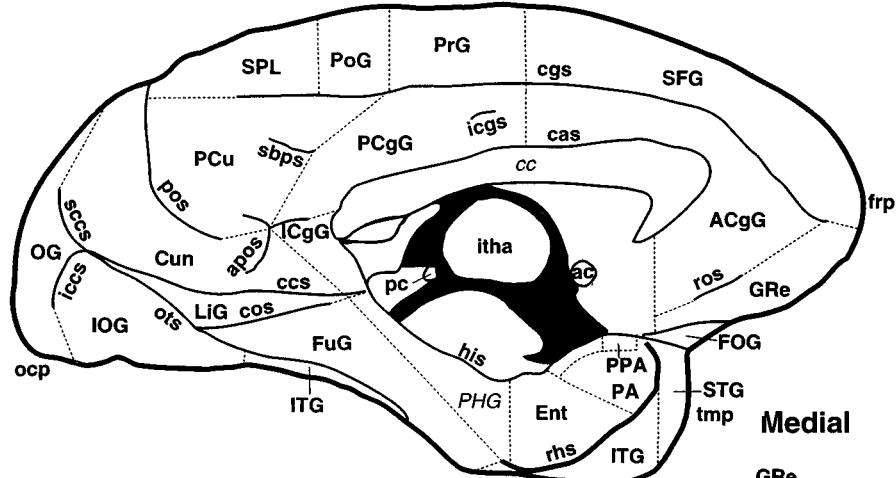
Atlas	Number of animals	Weight (g) (mean \pm SD or range)	Length (mm) (mean \pm SD or range)	Width (mm) (mean \pm SD or range)
Template Atlas	2	63.3	62	52
Szabo and Cowan (1984)	23	63.3 \pm 7.4	63.6 \pm 2.9	51 \pm 2.5
Shantha <i>et al.</i> (1968)	8	62–68	62–65	47–50



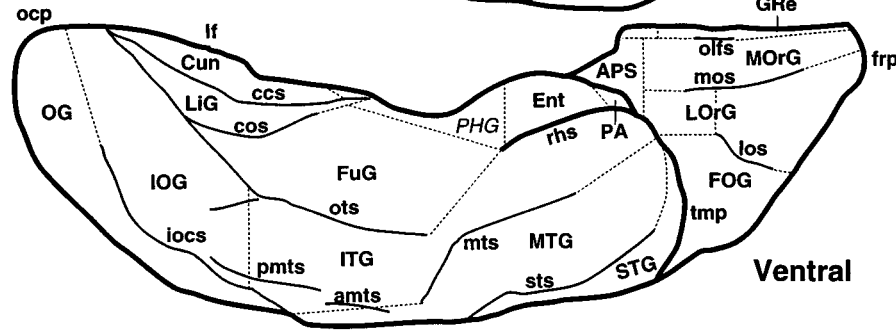
Lateral



Dorsal



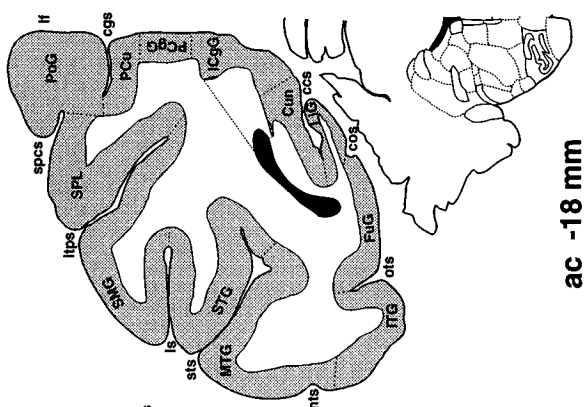
Medial



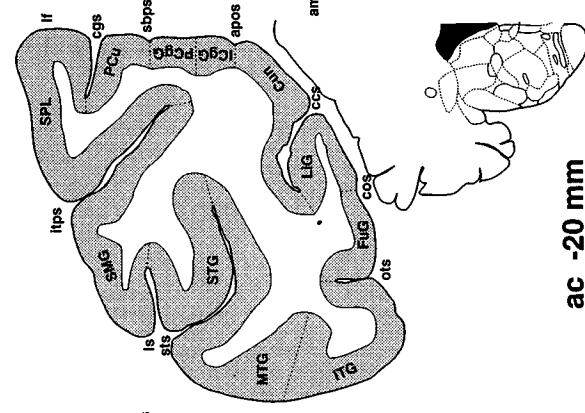
Ventral

- ac anterior commissure
- ACgG anterior cingulate gyrus
- amts anterior middle temporal sulcus
- AnG angular gyrus
- apos anterior parieto-occipital sulcus
- APS anterior perforated substance
- ascsc anterior subcentral sulcus
- cas callosal sulcus
- cc corpus callosum
- ccs calcarine sulcus
- cgs cingulate sulcus
- cos collateral sulcus
- cs central sulcus
- Cun cuneus
- ecs ectocalcarine sulcus
- Ent entorhinal area
- FOG fronto-orbital gyrus
- fros fronto-orbital sulcus
- frp frontal pole
- FuG fusiform gyrus
- GRe gyrus rectus
- his hippocampal sulcus
- iccs inferior calcarine sulcus
- ICgG isthmus of cingulate gyrus
- icgs intracingulate sulcus
- IFG inferior frontal gyrus
- Ins insula
- iocs inferior occipital sulcus
- IOG inferior occipital gyrus
- iras inferior ramus of arcuate sulcus
- ITG inferior temporal gyrus
- itha interthalamic adhesion
- itps intraparietal sulcus
- If longitudinal fissure
- LiG lingual gyrus
- LOrG lateral orbital gyrus
- los lateral orbital sulcus
- ls lateral sulcus
- lus lunule sulcus
- MFG middle frontal gyrus
- MORg medial orbital gyrus
- mos medial orbital sulcus
- MTG middle temporal gyrus
- mts middle temporal sulcus
- ocp occipital pole
- OG occipital gyrus
- ofs olfactory sulcus
- ots occipitotemporal sulcus
- PA periamygdaloid area
- pc posterior commissure
- PCgG posterior cingulate gyrus
- PCu precuneus
- PHG parahippocampal gyrus
- pmts posterior middle temporal sulcus
- PoG postcentral gyrus
- pos parieto-occipital sulcus
- PPA prepyriform area
- PrG precentral gyrus
- PrS presubiculum
- prs principal sulcus
- pscsc posterior subcentral sulcus
- rhs rhinal sulcus
- ros rostral sulcus
- sbps subparietal sulcus
- sccs superior calcarine sulcus
- SFG superior frontal gyrus
- SMG supramarginal gyrus
- spsc superior postcentral sulcus
- SPL superior parietal lobule
- sprsc superior precentral sulcus
- sras superior ramus of arcuate sulcus
- sts superior temporal sulcus
- STG superior temporal gyrus
- tmp temporal pole

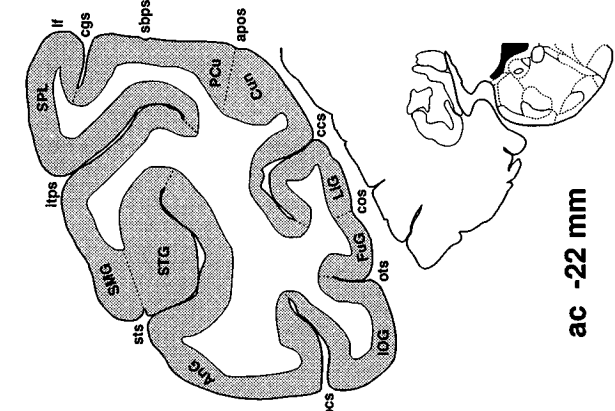
FIG. 2. Cerebral cortex of *M. fascicularis* as seen in lateral, dorsal, medial, and ventral views. The dotted boundaries are defined to as great an extent as possible by joining sulcal landmarks. The sulcal patterns are similar in the various macaque species.



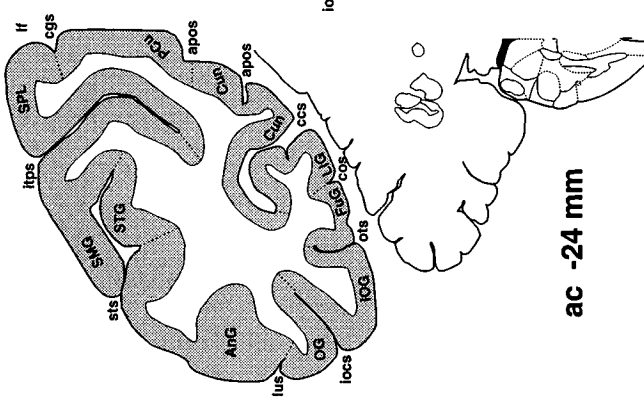
ac -18 mm



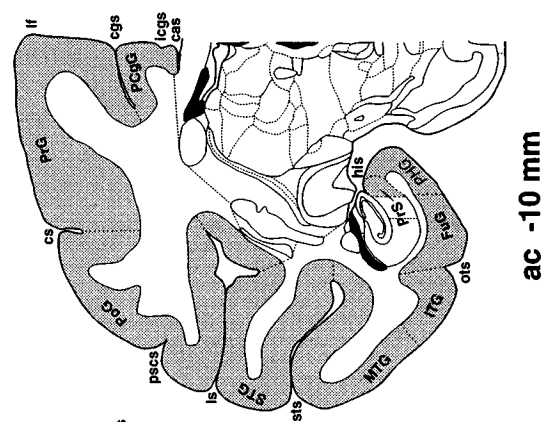
ac -20 mm



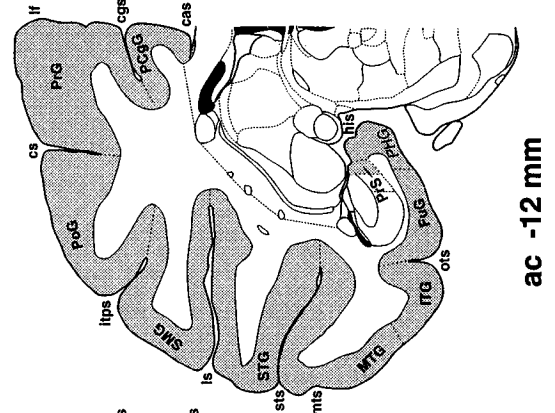
ac -22 mm



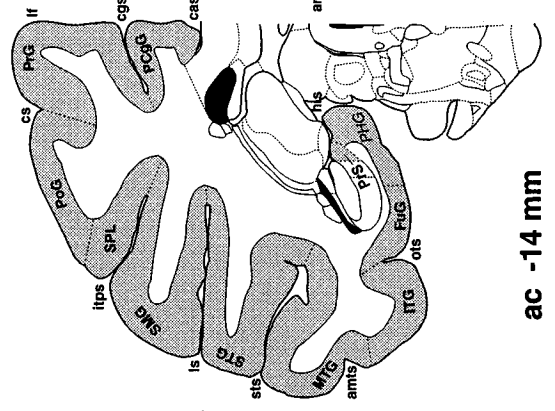
ac -24 mm



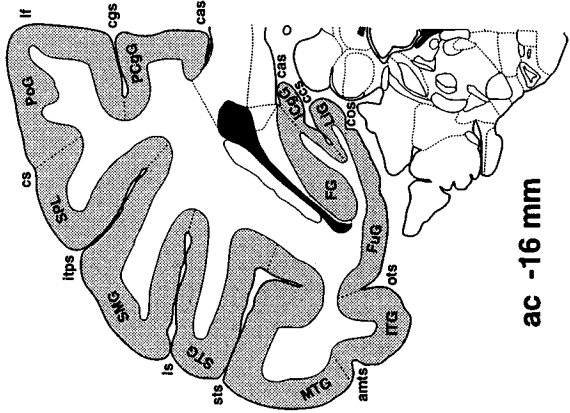
ac -10 mm



ac -12 mm



ac -14 mm



ac -16 mm

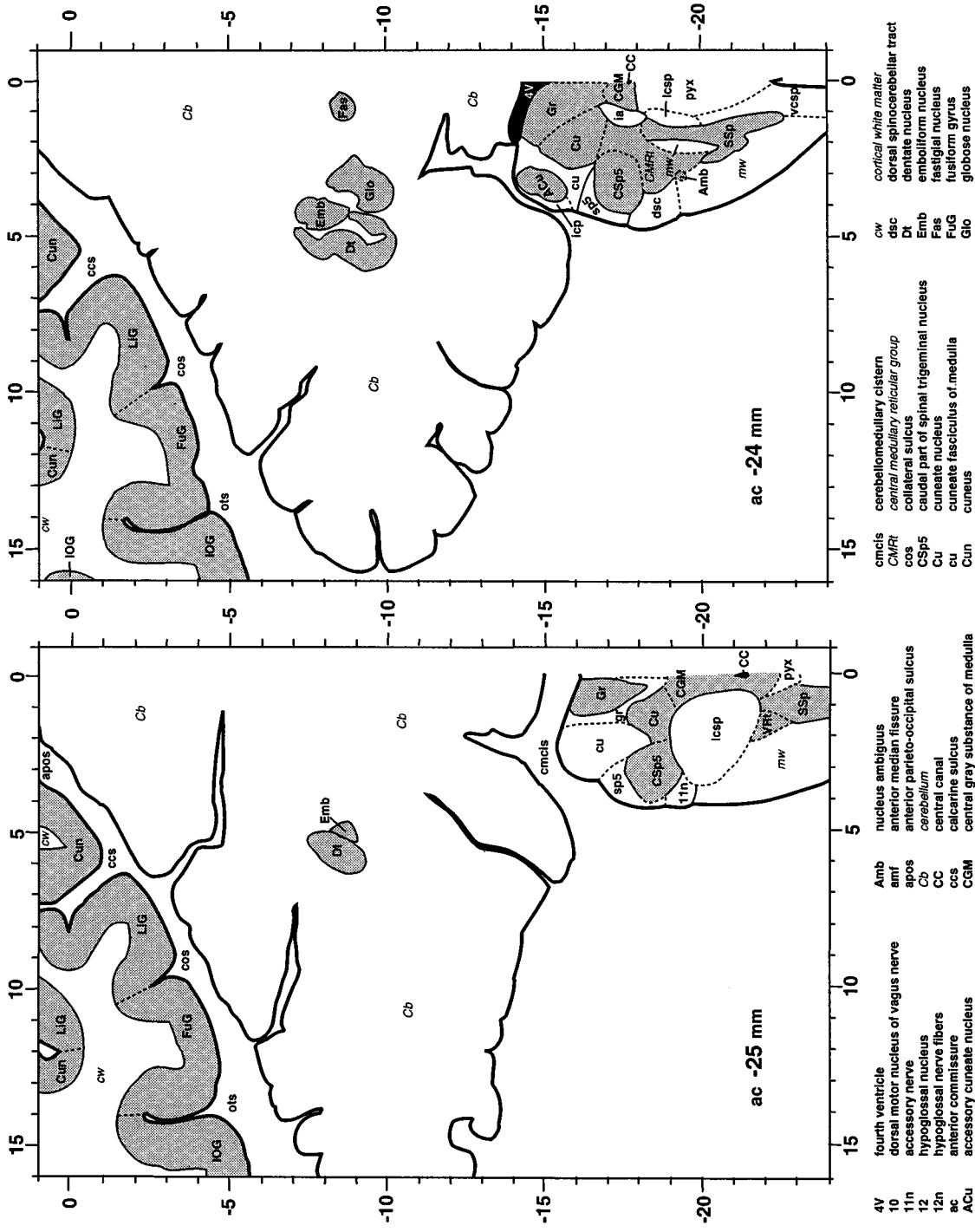
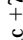
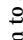
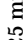



FIG. 4. Subcortical structures in *M. fascicularis* as seen in coronal sections at 1-mm intervals from ac -25 mm to ac +7 mm. Atlas conventions: Boundaries: —, an external boundary of the brain; — · —, an internal boundary readily visible directly or in a projected image of a stained section; - - - - -, a boundary that is either indistinct or arbitrary. A boundary is indistinct if detectable only by microscopy. It is arbitrary if it completes a boundary that is only partially definable because (1) a mixture of elements of adjacent structures changes gradually over a distance of more than about 200 μ m or (2) there is no cyto- or myeloarchitectural boundary. A prominent example of the latter is a boundary between cortical gyri completed by connecting sulcal landmarks. Shading: , a structure composed predominantly of gray matter (Nissl stained); , a structure composed predominantly of white matter (Weil stained); , a distinctive but unnamed (in the atlas) subdivision of a structure; , a cerebral ventricle. Labels, **bold plain text**, a primary structure; nonbold *italics*, an unsegmented "remainder" portion of a superstructure, some portion of which is shown as one or more independent primary structures; first letter capitalized, a structure which is predominantly cellular; first letter in lowercase, a structure which is predominantly myelinated, or a superficial feature such as a sulcus.

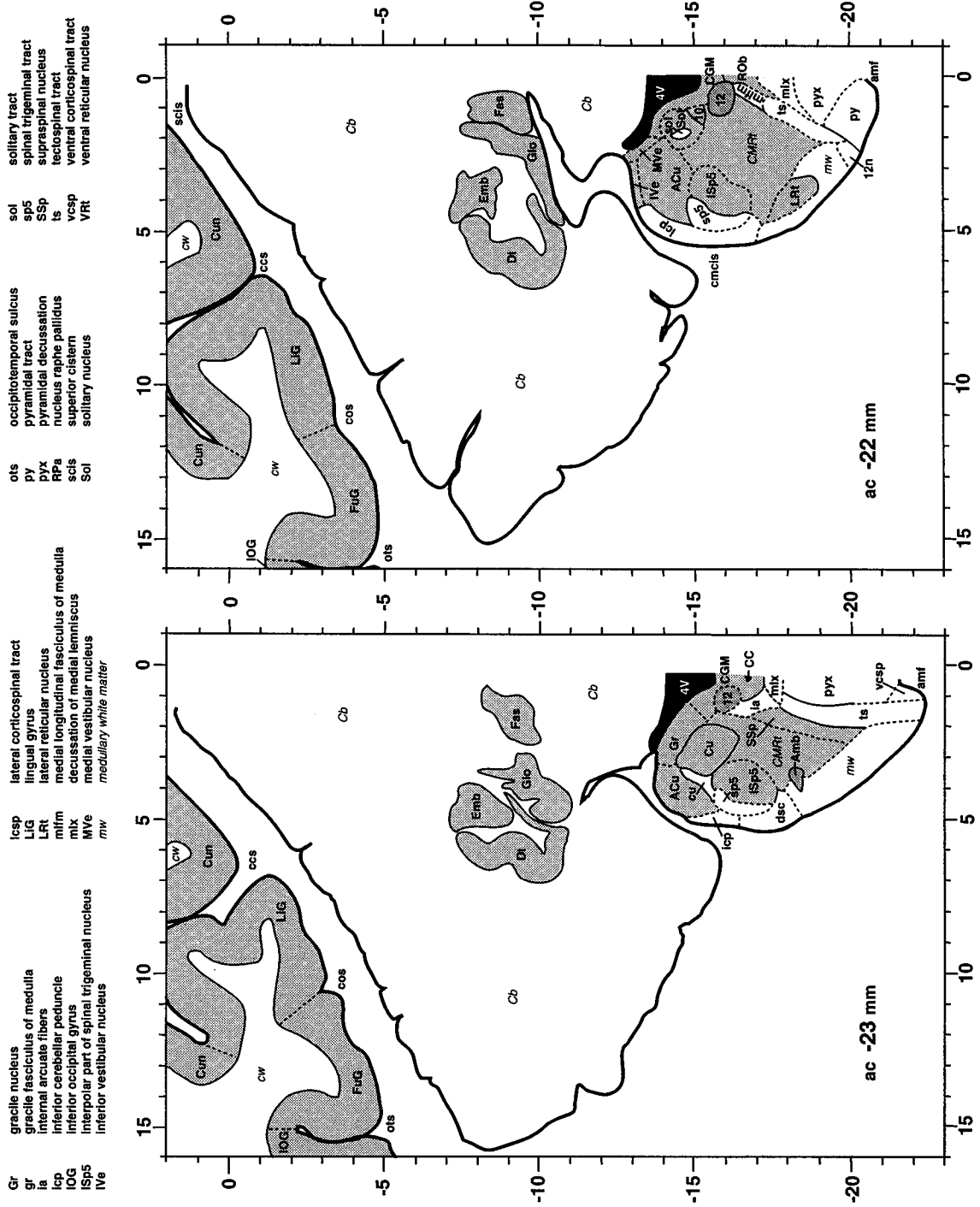


FIG. 4—Continued

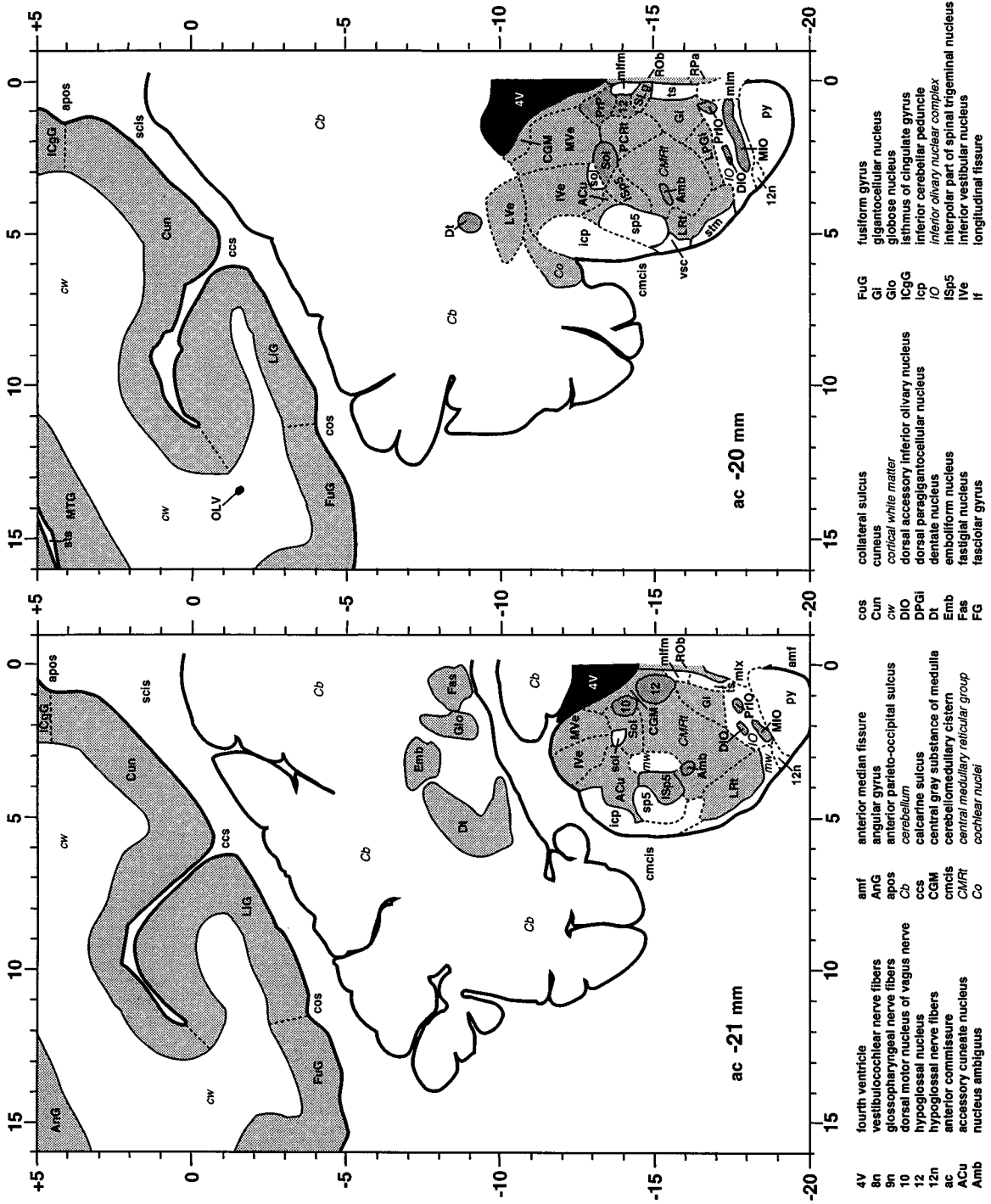


FIG. 4—Continued

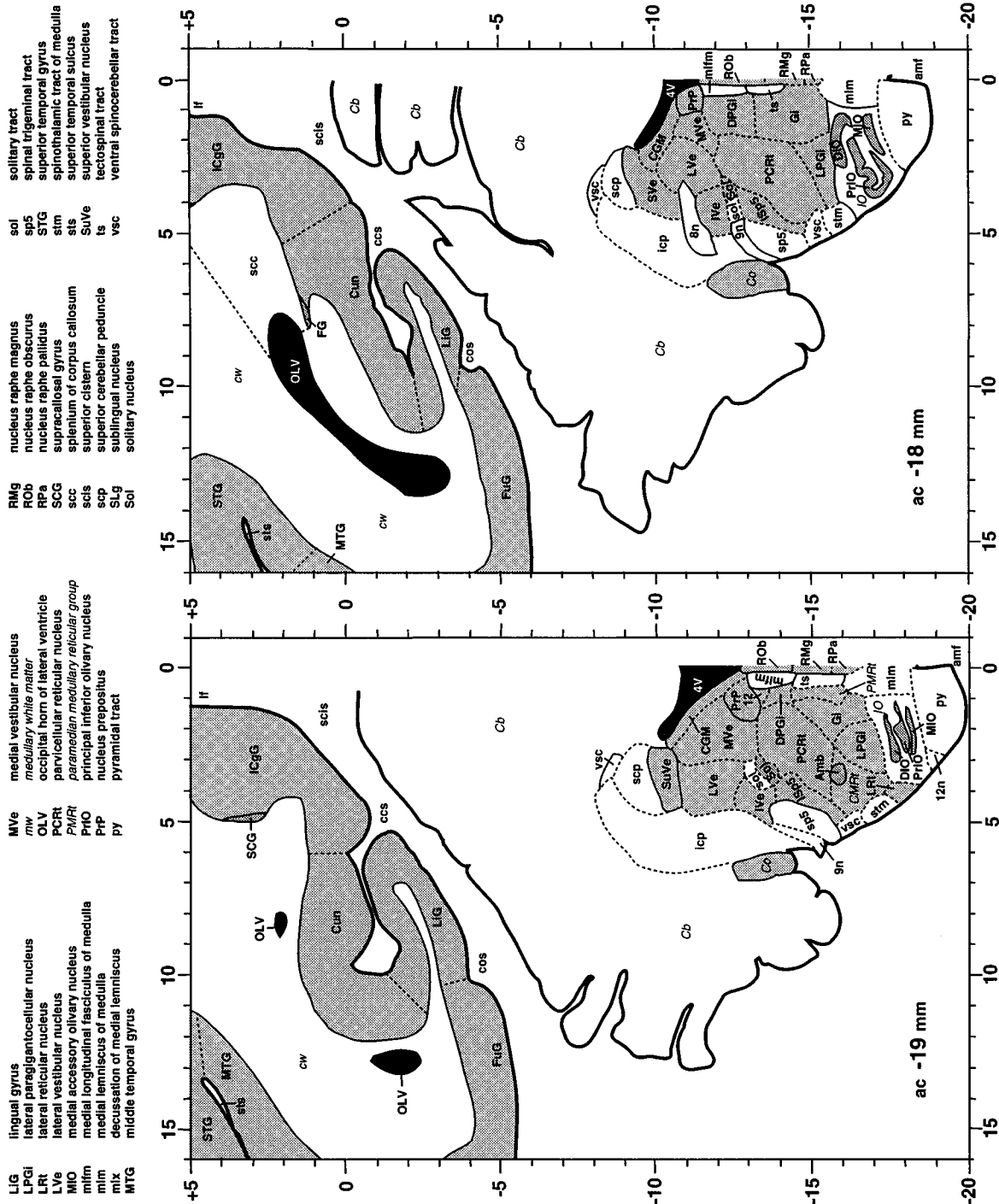


FIG. 4—Continued

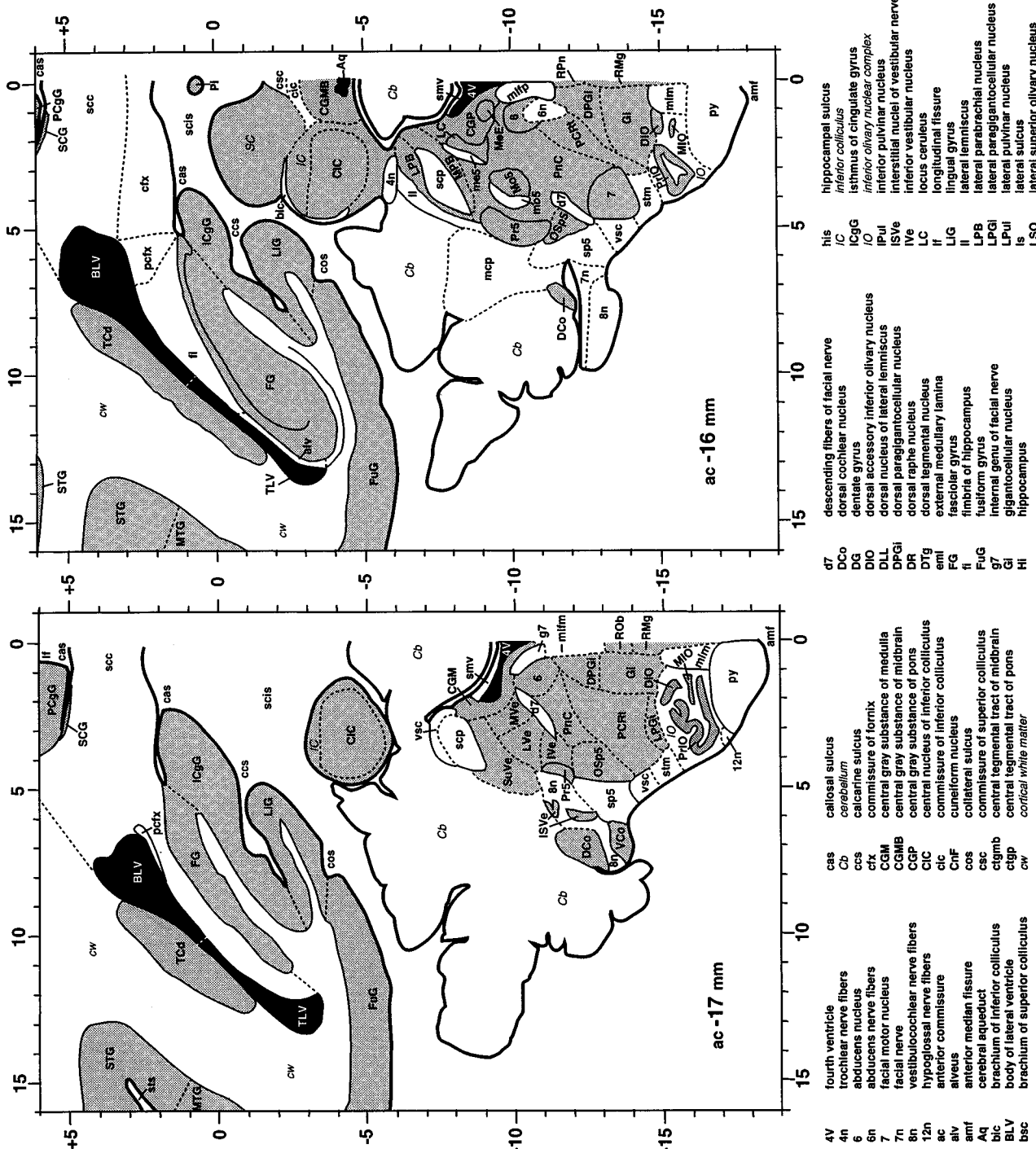


FIG. 4—Continued

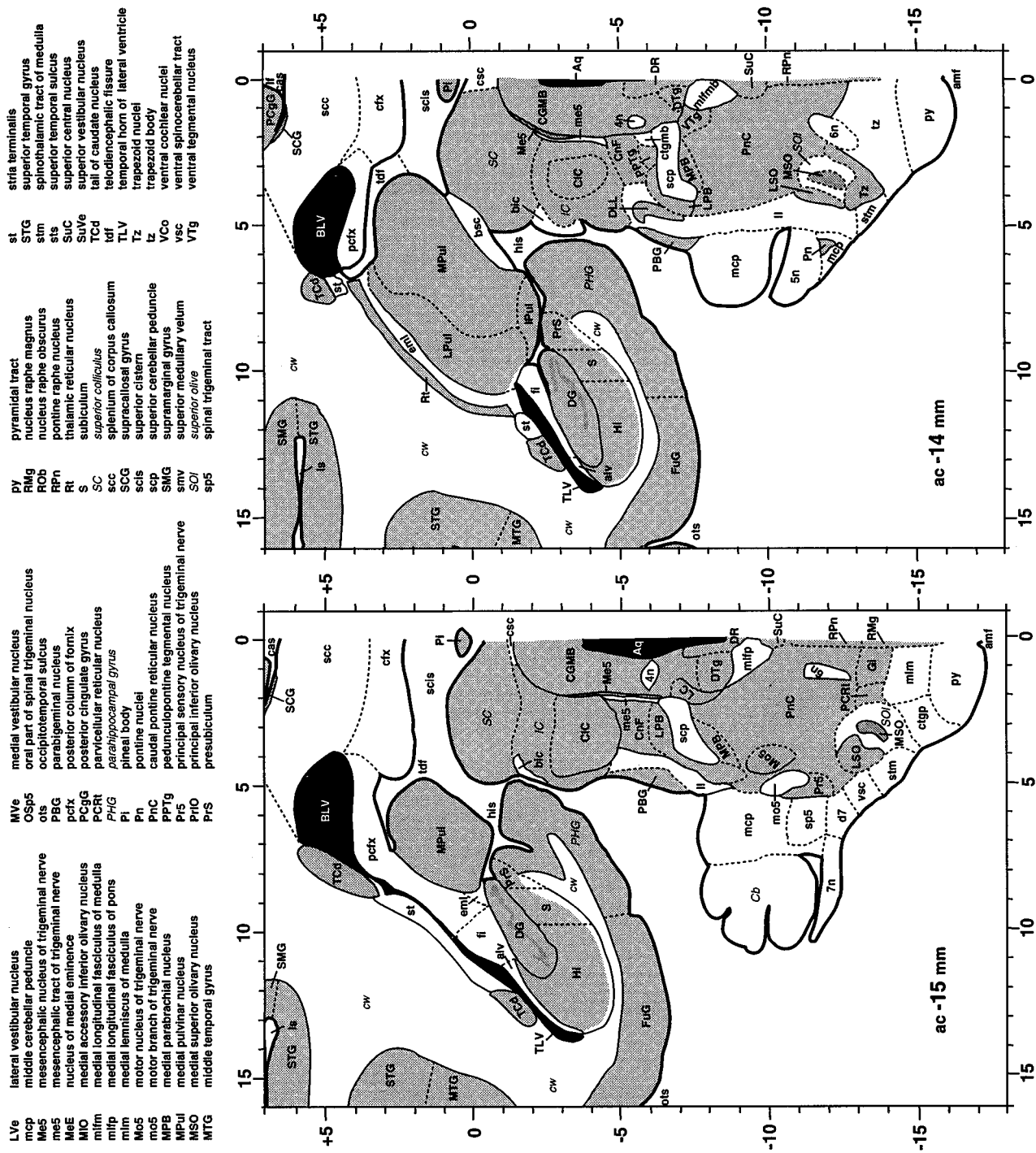


FIG. 4—Continued

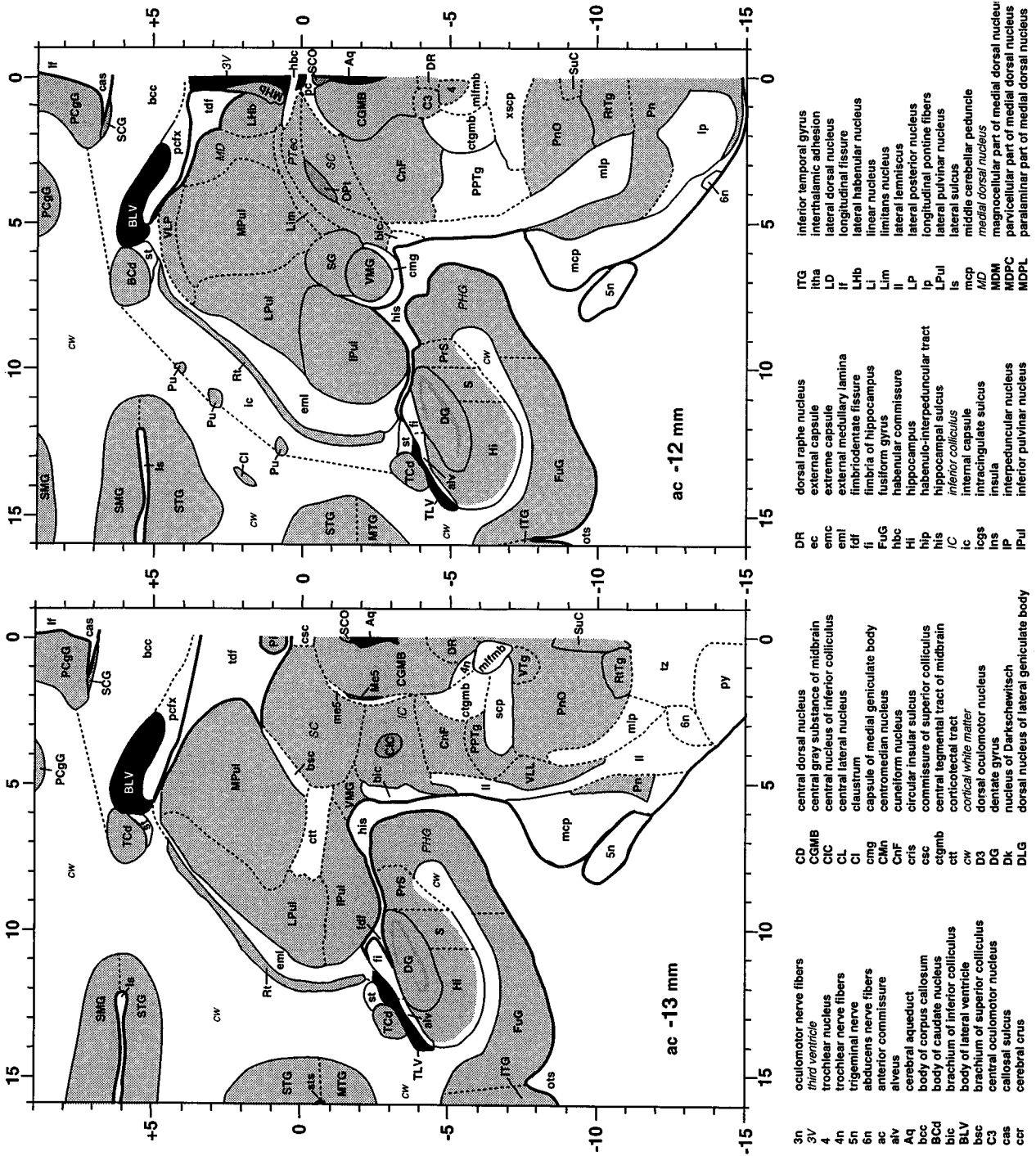


FIG. 4—Continued

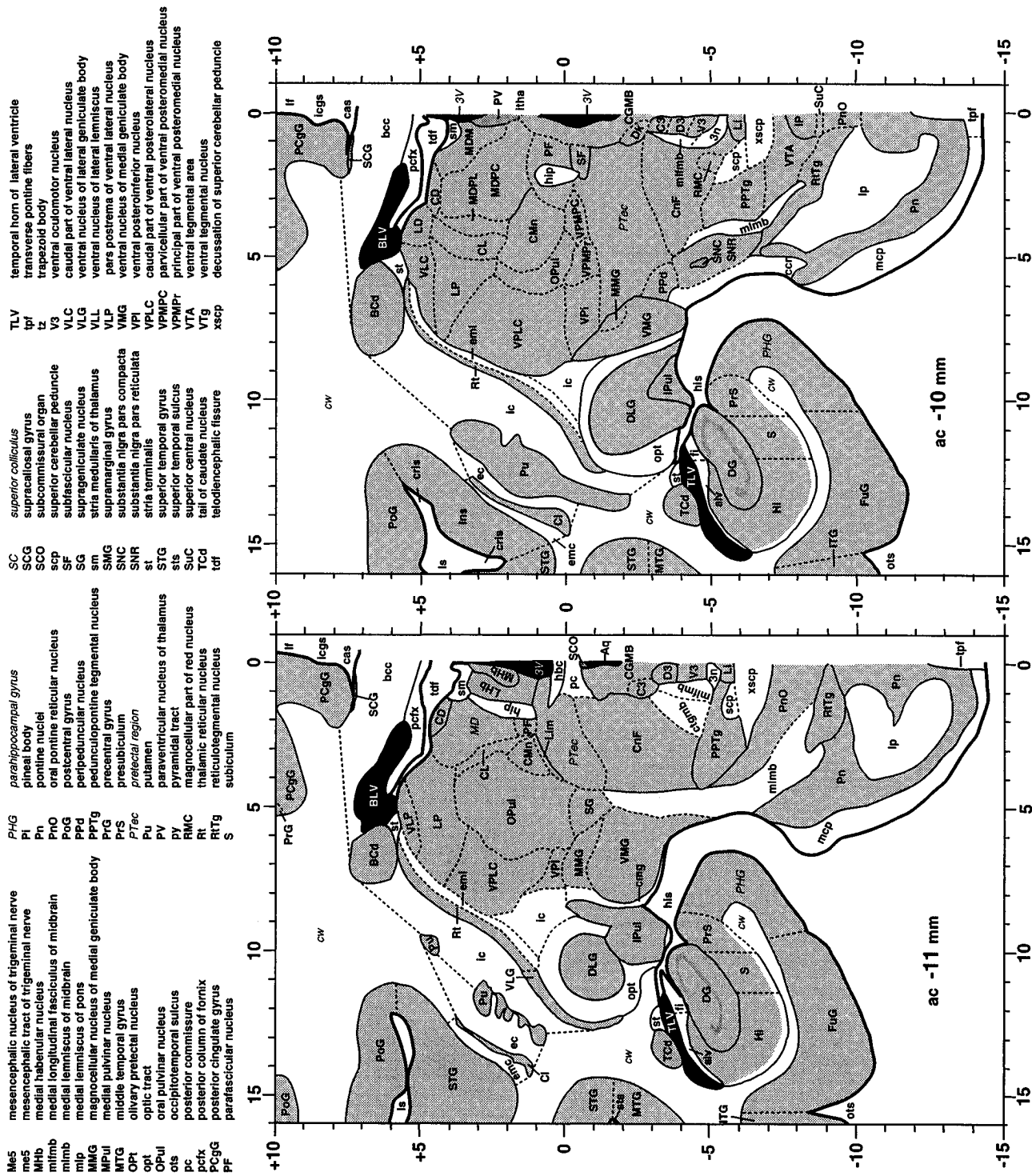


FIG. 4—Continued

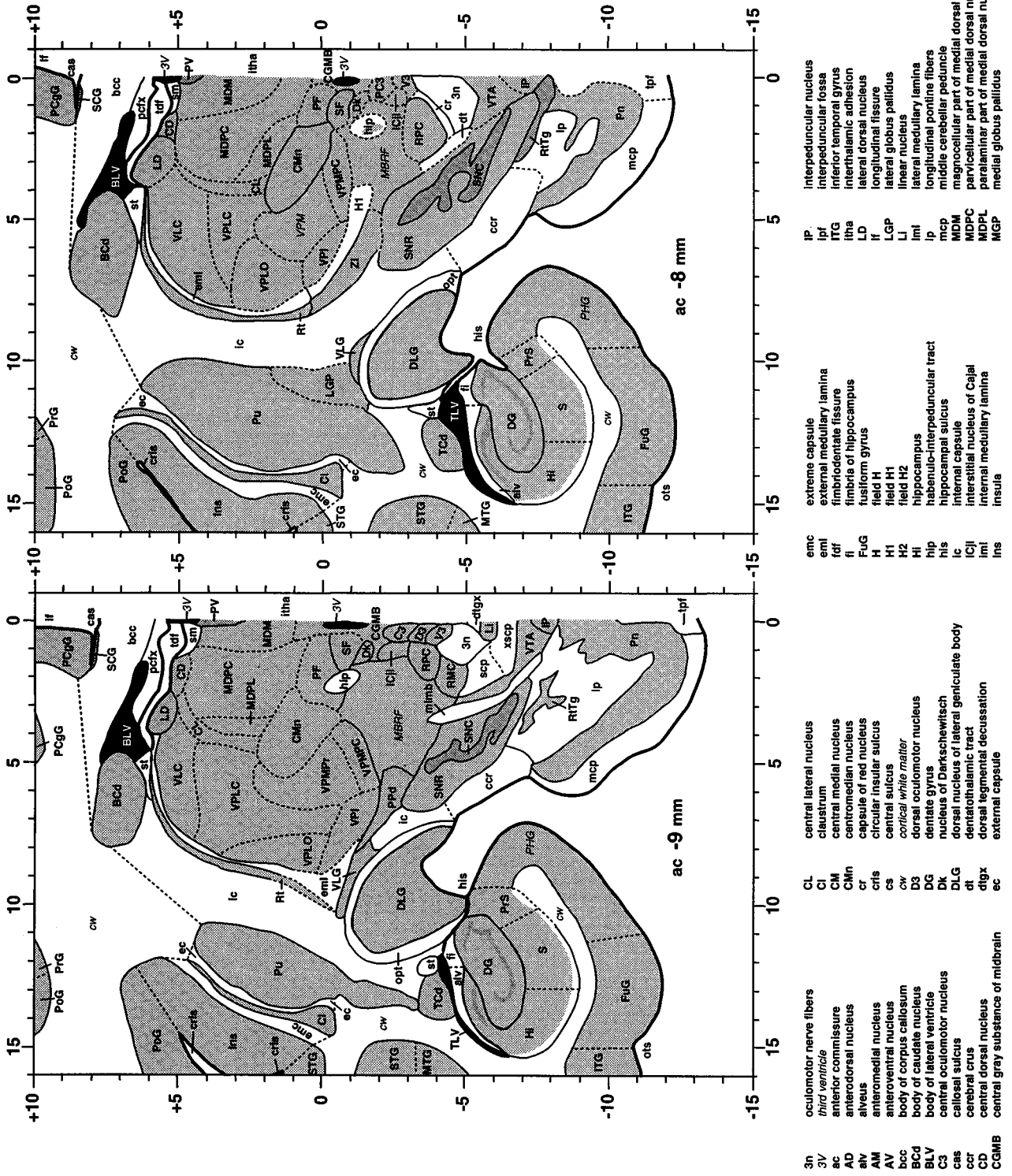


FIG. 4—Continued

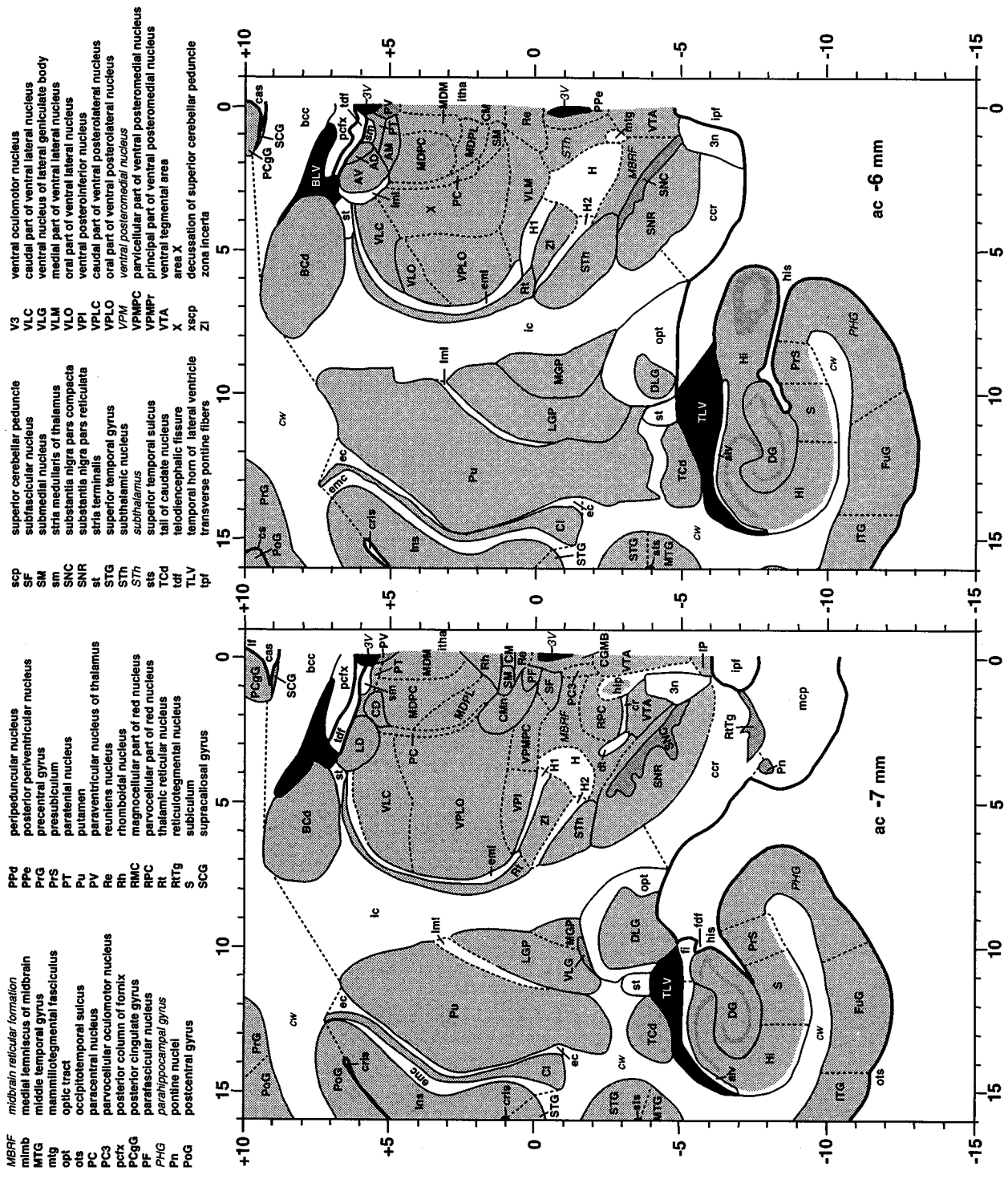


FIG. 4—Continued

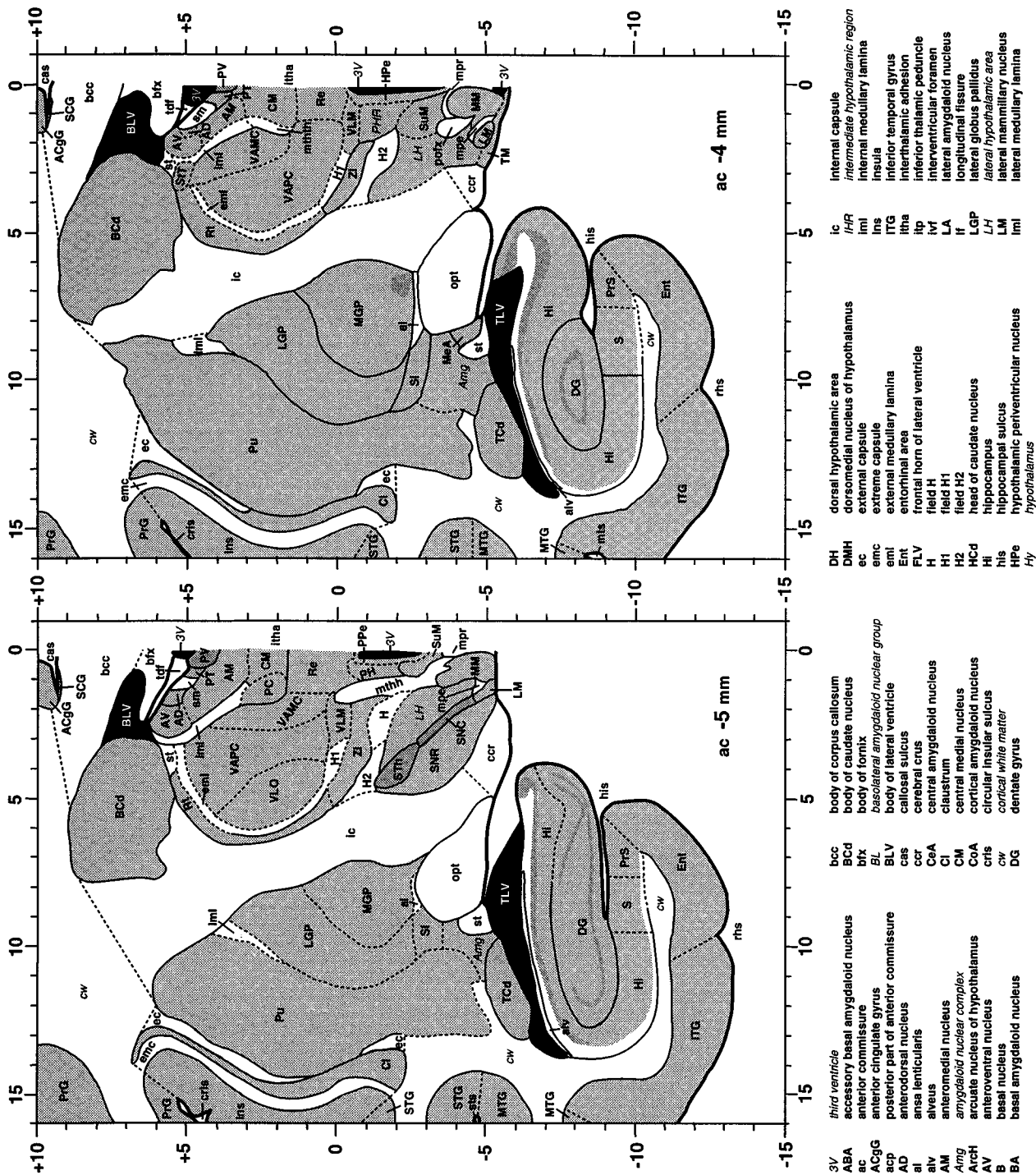


FIG. 4—Continued

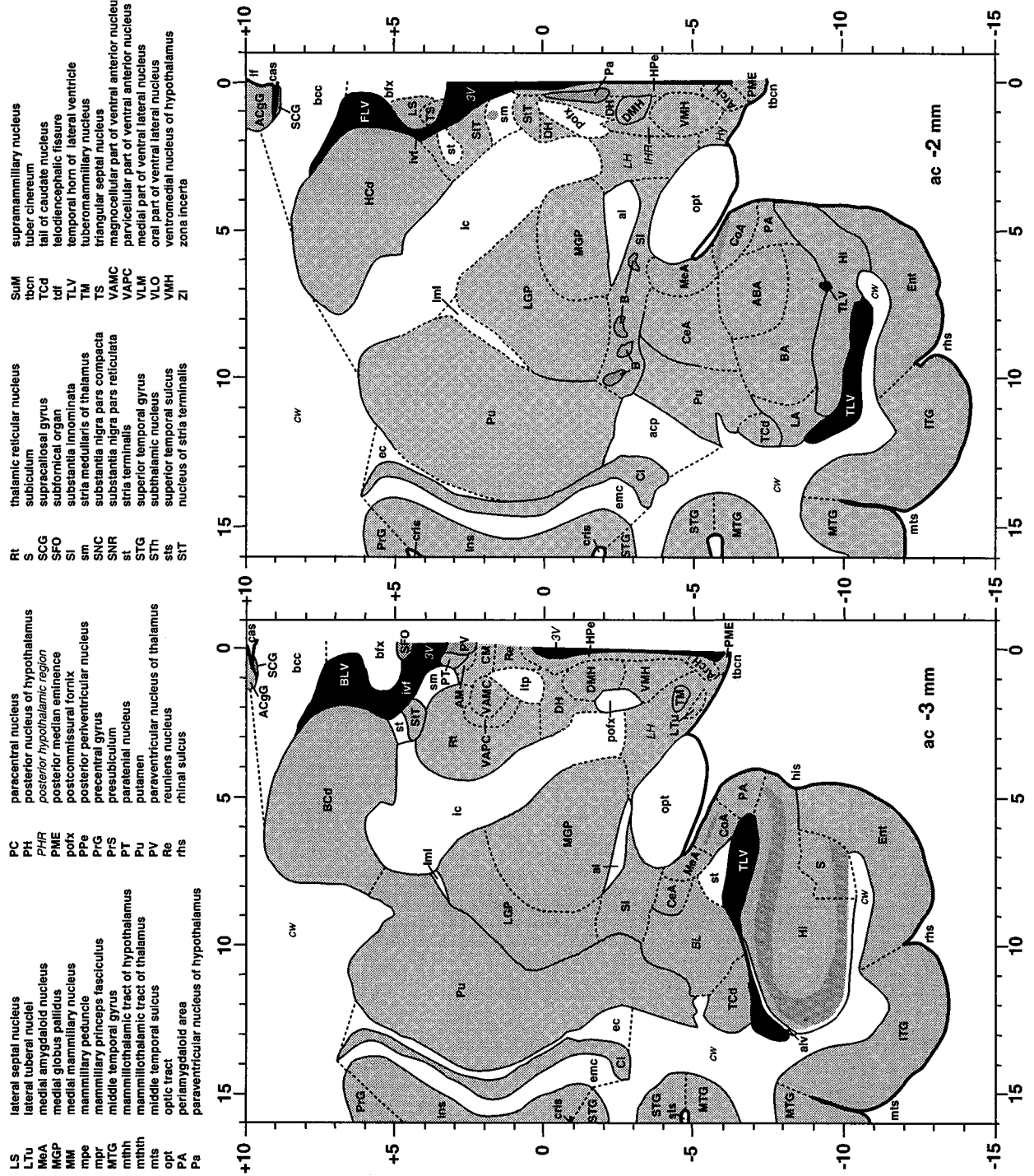


FIG. 4—Continued

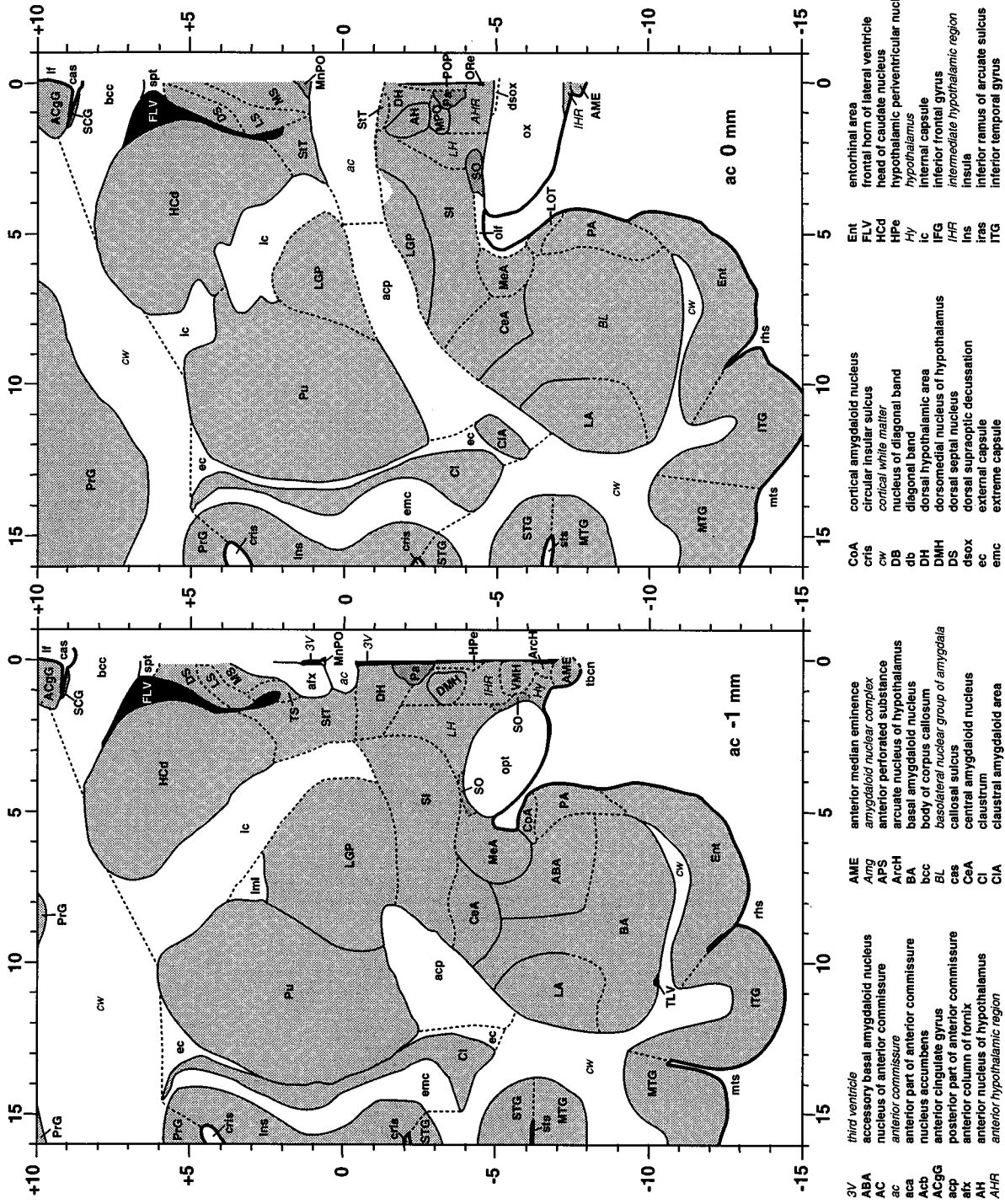


FIG. 4—Continued

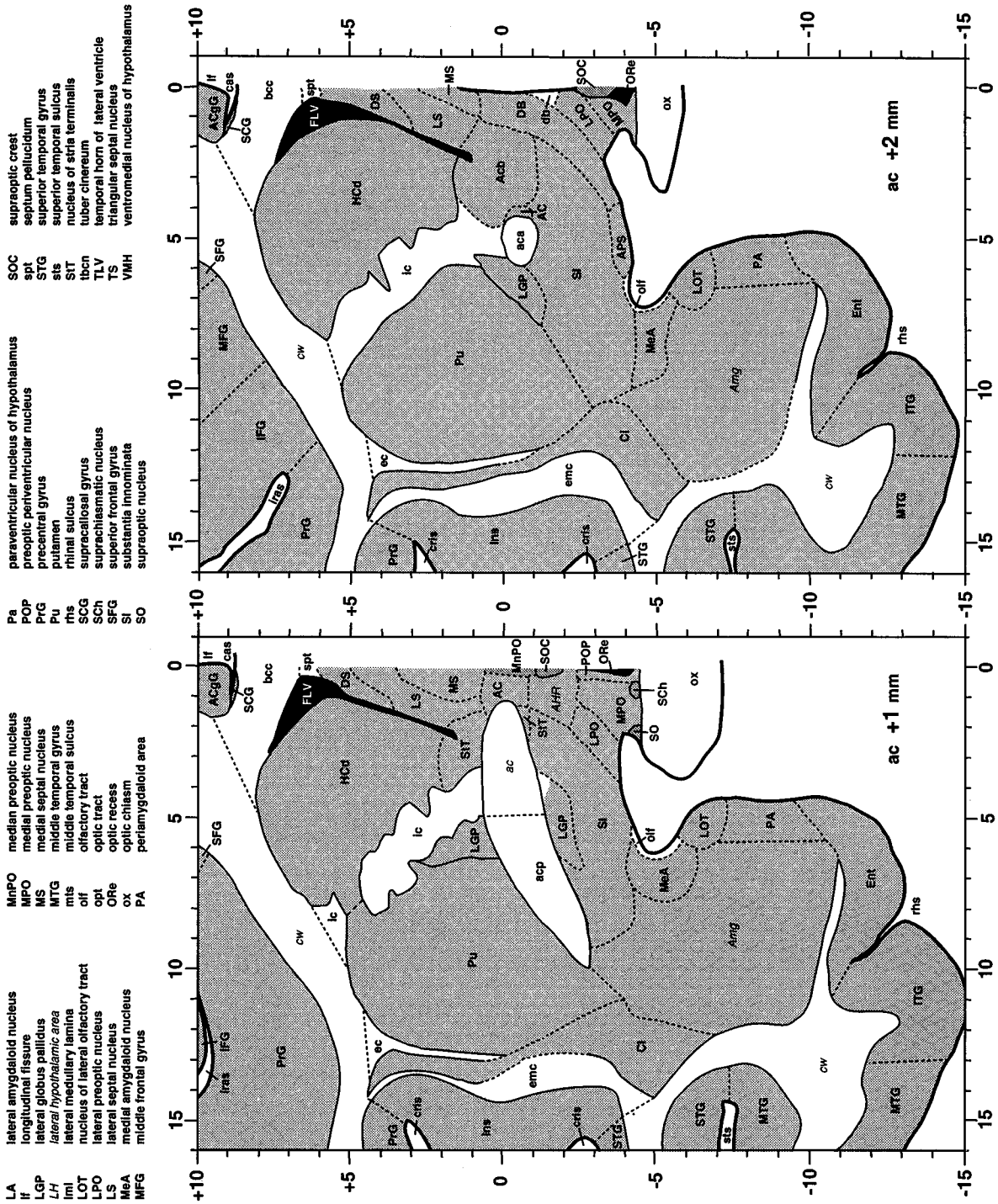


FIG. 4—Continued

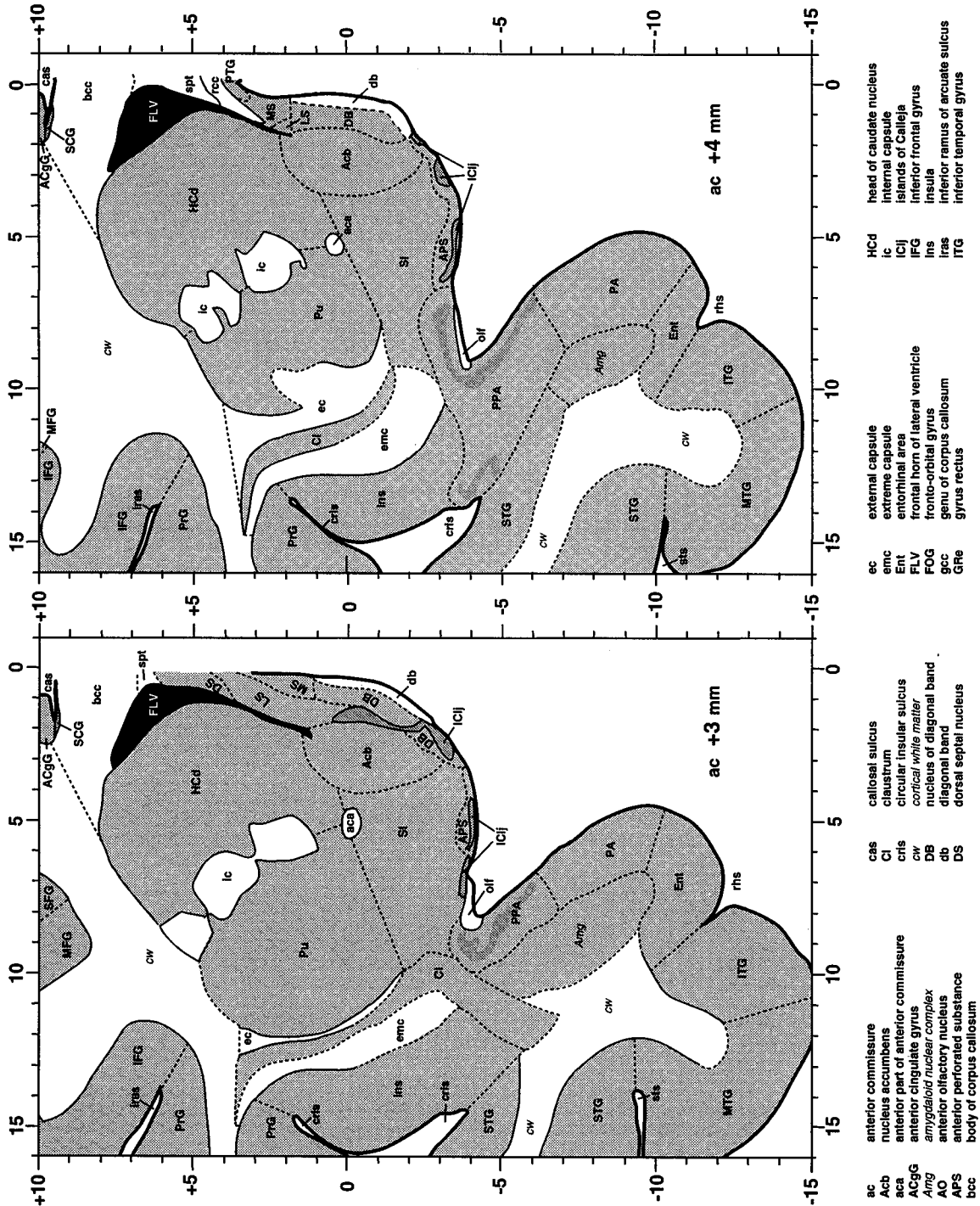


FIG. 4—Continued

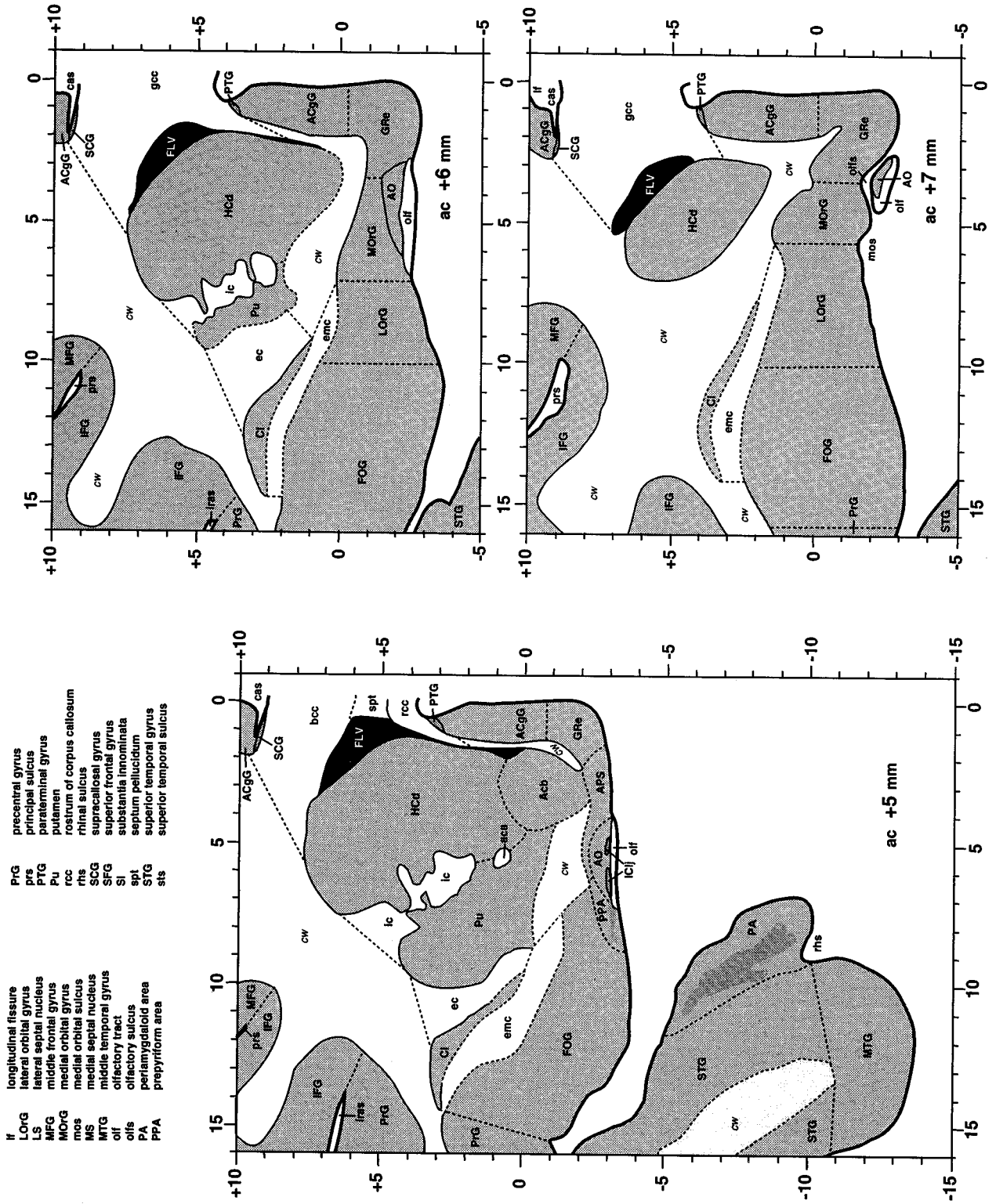


FIG. 4—Continued

nuclei, e.g., the abducens nucleus (6) and tail of the caudate nucleus at the level of the medial mammillary nucleus (TCD at AP of MM); the commissures, ac and pc; or cranial nerves, e.g., the trochlear nerve (4n), at their attachment to the brain stem. Other landmarks were the junctions of structures, such as the temporal and frontal lobes (TL/FL) and the opening of the central canal (CC) at the junction of the medulla with the spinal cord. If a structure extended through two or more coronal sections the AP coordinate of the center was defined as midway between the first and last sections in which it appeared.

Since the bicommissural line of the Szabo and Cowan atlas is very nearly parallel to the bicommissural line of the template brain (the DV coordinates of ac and pc are almost identical) the translation from the orbitomeatal space to bicommissural space was simple to calculate. We determined the difference between the AP coordi-

nate of ac in the conventional atlas and ac in the Template Atlas and added the difference to the AP of every landmark structure in the conventional atlas. The same operation was done to calculate the dorsoventral offset and to translate the DV coordinates of the structures to coordinates in bicommissural space. ML coordinates did not require translation, because the origin for ML coordinates was the same in both atlases, viz., the midline sagittal plane.

Not all coordinates were included for every landmark. For example, the ML coordinate of midline structures such as ac and interthalamic adhesion (IThA) was set by definition to 0.0 in both brains, so its inclusion in a test of fit between the two atlases would artificially inflate the impression of fit; likewise, the AP coordinate of the most dorsal point of cortex at the level of the anterior commissure (ctx top at AP of ac) was excluded, because it was fixed by definition. Other

TABLE 2

Comparison of Locations of Homologous Landmarks in the Template Atlas (TA) and Two Conventional Atlases (CA) of the *M. fascicularis* Brain

Landmark	Coordinate								
	Anteroposterior			Dorsoventral			Mediolateral		
	TA	CA ^a	diff	TA	CA ^a	diff	TA	CA ^a	diff
ac	0.0	0.0	0.0	0.0	0.0	0.0			
BCd at AP of pc				6.6	6.4	0.2	6.7	7.2	-0.5
CC (opening)	-22.5	-23.5	1.0	-16.5	-16.5	0.0			
ctx base at AP of				-15.3	-16.3	1.0			
ctx base at AP of				-15.0	-15.9	0.9			
ctx top at AP of				19.0	19.8	-0.8			
ctx top at AP of				19.0	19.0	0.0			
DLG	-8.0	-8.8	0.8	-3.2	-3.8	0.6	9.8	10.9	-1.1
Emb				-8.0	-7.2	-0.8	4.4	4.1	0.3
IO	-18.5	-18.4	-0.1	-17.2	-18.8	1.6	2.3	2.3	0.0
IP	-8.5	-8.9	0.4	-8.2	-8.6	0.4			
IThA	-6.5	-5.4	-1.1	2.6	2.4	0.2			
LC	-15.5	-15.9	0.4	-8.1	-9.2	1.1	2.1	2.3	-0.2
MM	-4.5	-4.1	-0.4	-4.5	-5.0	0.5			
MSO	-14.5	-14.4	-0.1	-13.0	-14.4	1.4	3.2	3.4	-0.2
ORe				-3.9	-3.1	-0.8			
ox	1.0	0.2	0.8	-6.8	-5.9	-0.9			
pc	-11.5	-10.9	-0.6	-0.3	0.0	-0.3			
Pu/SC junction	-14.5	-13.4	-1.1	0.2	-0.2	0.4	4.6	5.7	-1.1
rostral end of Hi				-8.4	-10.4	2.0	9.5	9.8	-0.3
STh	-6.0	-5.4	-0.6	-1.7	-3.2	1.5	4.3	5.1	-0.8
TCD at AP of M				-5.7	-6.6	0.9	11.5	11.8	-0.3
TL/FL junction	4.5	3.5	1.0	-4.3	-4.3	0.0	11.2	11.6	-0.4
6	-16.5	-16.9	0.4	-10.5	-11.6	1.1	1.2	1.2	0.0
10	-21.5	-20.9	-0.6	-14.6	-14.8	0.2	1.3	1.6	-0.3
4n (exit)	-16.0	-15.4	-0.6	-6.0	-6.2	0.2			
8n (exit)				-13.2	-14.0	0.8	7.0	7.6	-0.6
TA vs Szabo and Cowan (1984)		SD of diff	0.7			0.8			0.4
		% = or <1.0	88%			81%			86%
TA vs Shantha <i>et al.</i> (1968)		SD of diff	0.8			0.9			0.7
		% = or <1.0	80%			71%			79%

^a Individual coordinate data from Szabo and Cowan (1984) only.

coordinates were omitted, because they could not be determined with adequate precision. These included, for example, ML coordinates for the top and base of cortex (ctx base and ctx top) and the AP coordinate of the optic recess (ORe).

Comparing the coordinates of landmarks from the conventional atlas in bicommissural space with those of the same landmarks in the Template Atlas provided a measure of the degree of fit of the brain represented in the Template Atlas to that of the conventional atlas. The standard deviation of the differences in the AP dimension of the Szabo and Cowan (1984) atlas was 0.7 mm (Table 2). This indicated that for the 17 landmarks for which AP coordinates were compared, the standard deviation of differences in their coordinates was 0.7 mm. Assuming a normal distribution of differences, 68% of landmarks in the Template Atlas would be within 0.7 mm of the homologous point in the translated conventional atlas. In another way of looking at the same issue, 88% of the homologous landmarks were within 1.0 mm of each other in the AP dimension. There was no correlation between the magnitude of the difference and the location of the landmark along the AP axis, which suggested that the differences were not due to a systematic difference in the size of the brain on that axis. A large proportion of the differences in the AP coordinates may be attributable to measurement error, because, with a distance of about 1 mm between sections in both atlases, estimates on the AP axis could be accurate only to the nearest 0.5 mm. The standard deviation of differences in the DV dimension was 0.8 mm with 81% within 1.0 mm. The standard deviation in the ML dimension was 0.4 mm with 86% within 1.0 mm.

A similar comparison of the Template Atlas with the Shantha *et al.* (1968) atlas showed standard deviations of 0.7 to 0.9 mm with proportions of homologous landmarks within 1.0 mm ranging between 71 and 80% on the three dimensions. On the basis of these comparisons we conclude that the brain on which the Template Atlas is based was representative of *M. fascicularis* brains.

HOW TO USE THE TEMPLATE ATLAS

Any point in the computerized Template Atlas can be conveniently designated on alternative representations of the monkey brain, and vice versa, by the application of simple formulas derived and presented below. The formulas require only that the representation be acquired in such a way that one plane of its coordinate system coincides with the midline sagittal anatomical plane and that the coordinates of the anterior and posterior commissures be specified on that plane. These arrangements are described below for several alterna-

tive representations we have used, including X-ray ventriculograms and MRI.

X-Ray Ventriculogram

The procedures for obtaining and evaluating an X-ray ventriculogram to use with the Template Atlas are as follows. A lateral ventriculogram of the experimental brain is obtained with the animal in a stereotaxic instrument with elevated earbars and eyebars (Kopf). (Elevated earbars and eyebars provide a view of the cerebral ventricles unobstructed by the side bars of the instrument.) To assure that the X-ray beam is perpendicular to the midsagittal plane, it is aimed along the intermeatal line as defined by the overlapping shadows of the two earbars. In the resultant ventriculogram (Fig. 1B), the AP axis is drawn on the film as a line through the anterior commissure and parallel to a side bar of the instrument. The DV axis is drawn through the anterior commissure and perpendicular to the side bar.

All distances measured from these axes must be multiplied by a scale factor to compensate for the enlargement of the image on the film. This scale factor is equal to the distance from the X-ray source to the midsagittal plane, divided by the distance from the source to the film. The AP and DV coordinates of the anterior commissure of the experimental brain (eb) in bicommissural space ($APAC_{eb}$, $DVAC_{eb}$) are defined as 0, because the center of ac is the origin from which all other distances are measured. The AP coordinate of the posterior commissure ($APPC_{eb}$) is the measured distance from the posterior commissure to the DV axis, multiplied by the scale factor. Its sign is of course negative, since it always lies posterior to the anterior commissure. The DV coordinate of the posterior commissure ($DVPC_{eb}$) is the measured distance from the posterior commissure to the AP axis, multiplied by the scale factor. Its sign is positive if the posterior commissure lies above the AP axis, negative if below.

MRI

Procedures for obtaining and evaluating a series of MR images to use with the Template Atlas are as follows. The animal is placed in a nonferrous stereotaxic instrument equipped with earbars which contain a thin cylinder of MR-opaque substance at their core (e.g., Rebert *et al.*, 1991; Saunders *et al.*, 1990; Crist Instruments, Damascus, MD). The instrument, in turn, is placed in the MRI machine such that the ML axis of the stereotaxic instrument is level from side to side, and perpendicular to the long axis of the MRI chamber. The midsagittal MRI from such an arrangement is geometrically equivalent to a lateral ventriculogram and provides clear images of the anterior and posterior commissures (Fig. 1C). Coronal images, however, which

the machine automatically sets orthogonal to the midsagittal view, provide a more conveniently quantitative way to find $APAC_{eb}$, $DVAC_{eb}$, $APPC_{eb}$, and $DVPC_{eb}$. We find it convenient to use the "spoiled GRASS" (gradient recall acquisition in steady state) MRI format to generate a series of coronal images 1 mm apart. In our radiological facility, the field of view is set to 160 mm and each coronal image is converted to a TIF file containing 256×256 small squares designated as "pixels" by our imaging software (Photoshop; Adobe). Each pixel is therefore $160/256$ or $5/8$ mm on a side. The display also provides horizontal and vertical scale bars above and beside the image, calibrated in pixels. The coordinates of the anterior commissure ($APAC_{eb}$, $DVAC_{eb}$) are again defined as 0, because the anterior commissure lies at the origin from which any other distance is measured. The AP coordinate of the posterior commissure ($APPC_{eb}$) is the coronal section number of its image, minus the coronal section number of the image containing the anterior commissure. Its sign is again negative, since it always lies posterior to the anterior commissure. The DV coordinate of the posterior commissure ($DVPC_{eb}$) is its vertical scale value in its image, minus the vertical scale value of the anterior commissure in its image, multiplied by the pixel size. Its sign is positive if the posterior commissure is more dorsal than the anterior commissure, negative if more ventral.

Locating Sites from the Template Atlas in an Experimental Animal

The Template Atlas can be applied point-to-point to the brain of any experimental subject as portrayed in a lateral ventriculogram or an MRI series prepared as described above. This requires a change of three-dimensional coordinates from the bicommissural space of the Template Atlas to the coordinate system of the experimental brain. Since the midsagittal planes are coplanar, and since the origins at the anterior commissure are identical, the problem is reduced to rotation of a two-dimensional coordinate system about its origin (Taylor, 1959). To align the bicommissural line of the Template Atlas with the bicommissural line in the experimental brain, the Template Atlas must be rotated at ϕ through an angle ϕ :

$$\phi = \arctan(DVPC_{eb}/APPC_{eb}). \quad (1)$$

The effect of this rotation on any site S in the Template Atlas (APS_{TA} , DVS_{TA}) is expressed by the standard formulas for rotation of axes (Taylor, 1959):

$$APS_{eb} = APS_{TA} \times \cos(\phi) + DVS_{TA} \times \sin(\phi) \quad (2)$$

$$DVS_{eb} = -APS_{TA} \times \sin(\phi) + DVS_{TA} \times \cos(\phi), \quad (3)$$

where (APS_{TA} , DVS_{TA}) represent coordinates of the point in bicommissural space in the Template Atlas and (APS_{eb} , DVS_{eb}) represent coordinates of the same point in terms of the coordinate system of the experimental brain, in which the origin is at the anterior commissure and the bicommissural line has not been rotated.

For a point of interest in the Template Atlas, the corresponding point in the experimental brain can be found by applying Eqs. (2) and (3). On the lateral ventriculogram, the projection of this point can be found at APS_{eb} mm from the DV axis and DVS_{eb} mm from the AP axis. In the MRI series, this point can be found on the coronal section APS_{eb} mm from the coronal section containing the anterior commissure. On this section, the point lies at the pixel equivalent of DVS_{eb} mm from the anterior commissure pixel on the vertical scale. The ML value of the point in millimeters is unaffected by the difference in alignment, because the midsagittal planes of the two coordinate systems are coplanar:

$$MLS_{eb} = MLS_{TA}. \quad (4)$$

Locating Sites from an Experimental Animal in the Template Brain

Another common need is to determine the location in the Template Atlas of an injection site, stimulation site, implant, or lesion identified in the brain of an experimental animal. One has APS_{eb} , DVS_{eb} , and MLS_{eb} , the coordinates as measured in the lateral (AP/DV) and frontal (ML) ventriculograms, or as found in the MRI series, and one wishes to convert them to corresponding coordinates in the Template Atlas. For this purpose, the angle of rotation ϕ is determined by Eq. (1), and the following rearranged formulas (Taylor, 1959) are applied:

$$APS_{TA} = APS_{eb} \times \cos(\phi) - DVS_{eb} \times \sin(\phi) \quad (5)$$

$$DVS_{TA} = APS_{eb} \times \sin(\phi) + DVS_{eb} \times \cos(\phi). \quad (6)$$

Again, the ML values are unaffected:

$$MLS_{TA} = MLS_{eb}. \quad (7)$$

Use of the Template Atlas in Conventional Stereotaxic Procedures

The formulas described above allow a user of the Template Atlas to convert coordinates back and forth between the Atlas and an experimental brain as represented by ventriculography or MRI. These procedures are adequate for a wide range of applications. Users who wish to use the Atlas to conduct conventional

stereotaxic procedures, however, need to know how to relate the bicommissural coordinate system of the Atlas to the coordinate system of the stereotaxic instrument. Several investigators have described effective techniques for use of ventriculographic and MRI landmarks with conventional primate brain atlases. Their approaches are equally applicable to the Template Atlas and may suit the user's needs (Feger *et al.*, 1975; Ilinsky and Kultas-Ilinsky, 1982; Percheron, 1975; Saunders *et al.*, 1990).

We have found it useful under some circumstances to adjust the head of the animal in the stereotaxic instrument such that the bicommissural line of the animal is parallel to the horizontal plane of the stereotaxic instrument (Dubach *et al.*, 1985). With the brain so aligned, vertical tracks, e.g., of stimulating electrodes or injection cannulae, lie entirely in a plane parallel to the coronal sections of the Template Atlas. As they are advanced, such tracks pass successively through structures illustrated in a single page of the Atlas rather than moving at an angle from page to page. In reconstructing such tracks, if blocking of the brain is performed stereotaxically in a plane perpendicular to the bicommissural line, the tissue sections coincide with coronal sections in the Template Atlas. Likewise, it is convenient if brains prepared for comprehensive mapping of pathways or the distribution of neuromarkers are cut in a plane that parallels the planes of the coronal templates of the Atlas.

Rotation of the head to align the bicommissural plane parallel to the side bars requires adjustable eyebars (Dubach *et al.*, 1985). Also, two other points must be specified, namely, the location of earbar 0 (zero) in the midsagittal ventriculogram or MRI and the point of contact of the eyebars with the infraorbital ridge. Earbar 0, the intersection of the intermeatal line with the midsagittal plane, is highly variable because it is defined by bony landmarks outside the brain. It is nevertheless important in nonhuman primate stereotaxic neurosurgery, because it is the zero point on the AP scale of most, if not all, stereotaxic instruments, and because it is the fulcrum about which one rotates the brain to bring the bicommissural line into alignment with the stereotaxic instrument.

On the lateral ventriculogram, earbar 0 is the center point of the arc at the rounded upper end of the earbars. The AP coordinate of earbar 0 (APEZ_{eb}) is the measured distance from the DV axis to earbar 0 multiplied by the scale factor. The DV coordinate of earbar 0 (DVEZ_{eb}) is the measured distance from the AP axis to earbar 0, multiplied by the scale factor. (Note that both of the coordinates of earbar 0, APEZ_{eb} and DVEZ_{eb}, are negative in sign.)

In the MRI series, the earbars are marked on one coronal section by the MR-opaque substance at the core of the earbars. The AP coordinate of earbar 0 (APEZ_{eb})

is the coronal section number of its image, minus the coronal section number of the image containing the anterior commissure. The DV coordinate of earbar 0 (DVEZ_{eb}) is the vertical scale value at the medial tip of its image, minus the vertical scale value of the anterior commissure in its image, multiplied by the pixel size. The signs of APEZ_{eb} and DVEZ_{eb} are always negative, since earbar 0 always lies posterior and ventral to the anterior commissure.

The AP coordinate of the point of contact between the eyebars and the infraorbital ridge is determined directly from the stereotaxic instrument. With the animal mounted in the instrument, a pointer mounted on the side bar of the instrument is used to determine EY_{eb}, i.e., the AP distance from the AP level of the earbar 0 to the AP level of the points on the eyebars that contact the inferior orbital ridge.

The coordinates APEZ_{eb} and DVEZ_{eb}, and the distance EY_{eb}, are used to calculate ADJ, the distance the eyebars must be adjusted up or down to align the bicommissural line of the animal parallel with the side bar of the stereotaxic instrument.

A largely graphical solution to the problem of determining ADJ has been previously presented (Dubach, 1991).³ While the graphical solution is suited to ventriculography, it involves making several additional measurements by hand, and it is not practical with MRI. Thus, we present a more fully algebraic solution. This solution, despite its rather complicated formula, is simpler than the graphical solution in terms of the inputs it requires. The formulas can easily be entered on a spreadsheet for efficient calculation of ADJ at surgery.

$$ZA = \text{SQRT} [(APEZ_{eb} - APAC_{eb})^2 + (DVEZ_{eb} - DVAC_{eb})^2], \quad (8)$$

where ZA is the distance from earbar 0 to the anterior commissure.

$$ZP = \text{SQRT} [(APPC_{eb} - APEZ_{eb})^2 + (DVPC_{eb} - DVEZ_{eb})^2], \quad (9)$$

where ZP is the distance from earbar 0 to the posterior commissure.

$$PA = \text{SQRT} [(APPC_{eb} - APAC_{eb})^2 + (DVPC_{eb} - DVAC_{eb})^2], \quad (10)$$

³ The graphical solution in the publication cited contains a misprint in the caption to Fig. 2. A5 should equal the square root of (A3² - HA²), not the square root of (A3² × HA²) as published.

where PA is the distance between the posterior commissure and the anterior commissure.

$$\alpha = \arccos [(ZP^2 - PA^2 - ZA^2)/(-2 \times PA \times ZA)], \quad (11)$$

where α is the angle between the bicommissural line and the line defined by earbar 0 and the anterior commissure.

$$EZtoBL = ZA \times \sin(\alpha), \quad (12)$$

where EZtoBL is the distance from earbar 0 to the bicommissural line.

$$SLOPE_{BL} = (DVPC_{eb} - DVAC_{eb})/(APPC_{eb} - APAC_{eb}), \quad (13)$$

where $SLOPE_{BL}$ is the tangent of the angle through which the head must be rotated to align the bicommissural line parallel to the horizontal plane of the stereotaxic instrument.

$$ACtoEY = EY_{eb} + APEZ_{eb}, \quad (14)$$

where ACtoEY is the distance from the AP level of the anterior commissure to the eyebar, along the orbitomeatal line; i.e., the line between the eyebar and earbar 0.

$$EYtoBL = (ACtoEY \times SLOPE_{BL}) - DVEZ_{eb}, \quad (15)$$

where EYtoBL is the distance between the eyebar and the bicommissural line, along a line perpendicular to the orbitomeatal line. Finally,

$$ADJ = EZtoBL - EYtoBL. \quad (16)$$

The eyebars should be adjusted up if ADJ is positive in sign, down if it is negative.

The rotation of axes about earbar 0 of course alters the positions of the anterior and posterior commissures relative to earbar 0. The rotation has oriented the brain in bicommissural space of the Template Atlas, with the bicommissural line on the AP axis and the anterior commissure at the origin. In this space, the coordinates of the anterior commissure are

$$APAC_{TA} = 0.0 \quad (17)$$

$$DVAC_{TA} = 0.0, \quad (18)$$

coordinates of the posterior commissure are

$$APPC_{TA} = -PA \quad (19)$$

$$DVPC_{TA} = 0.0, \quad (20)$$

and coordinates of earbar 0 are

$$APEZ_{TA} = -SQRT(ZA^2 - EZtoBL^2), \quad (21)$$

$$DVEZ_{TA} = -EZtoBL. \quad (22)$$

So rotated, coronal sections of the brain of the experimental animal coincide with coronal sections in the Template Atlas. Within the limits of measurement error and individual variation, any point in the experimental brain, with coordinates measured stereotaxically from the anterior commissure, will coincide with the point of the same coordinates in the Template Brain.

Collation and Illustration of Neuroanatomical Data from Multiple Animals

A further anticipated use of the Template Atlas is for standardized reporting and illustration of neuroanatomical data from multiple animals. The comprehensive segmentation of sections from most regions of the brain provides a useful template on which to record the location of a variety of data. This might include, for example, the locations of labeled neurons, injection sites, electrical stimulation sites, neurophysiological recording sites, or lesions. Usually such data are obtained from a stained section of the brain which provides many more landmarks for locating homologous locations in the Template Atlas than are provided by either ventriculography or MRI. Thus, while Eqs. (5)–(7) could be used to transfer such information from multiple animals to corresponding sections from the Template Atlas, the transfer will usually be done more accurately by hand or by a warping routine for digitized images to take advantage of the multiple landmarks (e.g., Bookstein and Green, 1994; Toga, 1994). A set of templates for this purpose, i.e., drawings which show the boundaries of structures without stereotaxic scale, shading, or labels and which include the cortical portion of each section, has been produced from the Illustrator files described above.⁴

ACKNOWLEDGMENTS

The authors express their appreciation to Orville Smith for lending his neuroanatomical expertise, his library, and his continual support and encouragement to their pursuit of the Template Atlas project; Mark Dubach for insightful suggestions and assistance in stereotaxic trigonometry; the Primate Information Center for its comprehensive bibliography of primate brain atlases; Michael Shadlen for the MRI illustration; and Kate Elias for her editorial assistance. This research was supported by USPHS Grant RR-00166 to the Regional Primate Research Center at the University of Washington.

⁴ Available as "Template Brain" from the Primate Information Center, Box 357330, University of Washington, Seattle, WA 98195 [telephone (206) 543-4376; E-mail: pic@bart.rprc.washington.edu].

REFERENCES

- Alvarez-Royo, P., Clower, R. P., Zola-Morgan, S., and Squire, L. R. 1991. Stereotaxic lesions of the hippocampus in monkeys: Determination of surgical coordinates and analysis of lesions using magnetic resonance imaging. *J. Neurosci. Methods* **38**:223–232.
- Amaral, D. G., Price, J. L., Pitkanen, A., and Carmichael, S. T. 1992. Anatomical organization of the primate amygdaloid complex. In *The Amygdala: Neurobiological Aspects of Emotion, Memory and Mental Dysfunction*, pp. 1–66. Wiley-Liss, New York.
- Anthony, T. R. 1994. *Neuroanatomy and the Neurologic Exam: A Thesaurus of Synonyms, Similar-Sounding Non-Synonyms, and Terms of Variable Meaning*. CRC Press, Boca Raton, FL.
- Benevento, L. A. 1975. Stereotaxic coordinates for the rhesus monkey thalamus and mesencephalon referencing visual afferents and cytoarchitecture. *J. Hirnforsch.* **16**:117–129.
- Bleier, R. 1984. *The Hypothalamus of the Rhesus Monkey: A Cytoarchitectonic Atlas*. Univ. of Wisconsin Press, Madison.
- Bonin, G. V., and Bailey, P. 1947. *The Neocortex of Macaca mulatta*. Univ. of Illinois Press, Urbana.
- Bookstein, F. L., and Green, W. D. K. 1994. Edgewarp: A flexible program package for biometric image warping in two dimensions. In *Visualization in Biomedical Computing* (R. A. Robb, Ed.), pp. 135–147. SPIE—Int. Soc. Opt. Eng., Bellingham, WA.
- Bowden, D. M. 1989. Trends in species studied by neuroscientists 1973–1988. *Neurosci. News* **20**:4–5.
- Bowden, D. M., and Martin, R. F. 1995. NeuroNames brain hierarchy. *Neuroimage* **2**:63–83.
- Bowden, D. M., and Martin, R. F. 1996. A digital Rosetta stone for primate brain terminology. In *Handbook of Chemical Neuroanatomy* (A. Bjorklund and T. Hokfelt, Eds.). Elsevier, Amsterdam. In press.
- Bowden, D. M., German, D. C., and Poynter, W. D. 1978. Autoradiographic stereotaxic mapping of axons originating in locus ceruleus and adjacent nuclei of *Macaca mulatta*. *Brain Res.* **145**:257–276.
- Brinkley, J. F., Eno, K., and Sundsten, J. W. 1993. Knowledge-based client-server approach to structural information retrieval: The Digital Anatomist Browser. *Comput. Methods Programs Biomed.* **40**:131–145.
- Carpenter, M. B., and Sutin, J. 1983. *Human Neuroanatomy*. Williams and Wilkins, Baltimore.
- Crosby, E. C., Humphrey, T., and Lauer, E. W. 1962. *Correlative Anatomy of the Nervous System*. MacMillan Co., New York.
- Downs, J. H., Lancaster, J. L., and Fox, P. T. 1994. Three-dimensional surface-based spatial normalization using a convex hull. In *Functional Neuroimaging: Technical Foundations* (R. W. Thatcher, M. Hallett, T. Zeffiro, E. R. John, and M. Huerta, Eds.), pp. 131–136. Academic Press, San Diego.
- Dubach, M. 1991. Accurate stereotaxic injection by radially curved injection needles. *Neurosurgery* **29**:144–149.
- Dubach, M. F., Tongen, V. C., and Bowden, D. M. 1985. Techniques for improving stereotaxic accuracy in *Macaca fascicularis*. *J. Neurosci. Methods* **13**:163–169.
- Emmers, R., and Akert, K. 1963. *A Stereotaxic Atlas of the Brain of the Squirrel Monkey (Saimiri sciureus)*. Univ. of Wisconsin Press, Madison.
- Feger, J., Ohye, C., Gallouin, F., and Albe-Fessard, D. 1975. Stereotaxic technique for stimulation and recording in nonanesthetized monkeys: Application to the determination of connections between caudate nucleus and substantia nigra. In *Advances in Neurology* (B. S. Meldrum and C. D. Marsden, Eds.), pp. 35–45. Raven Press, New York.
- German, D. C., and Bowden, D. M. 1974. Catecholamine systems as the neural substrate for intracranial self-stimulation: A hypothesis. *Brain Res.* **73**:381–419.
- German, D. C., and Bowden, D. M. 1975. Locus ceruleus in rhesus monkey (*Macaca mulatta*): A combined histochemical fluorescence, Nissl and silver study. *J. Comp. Neurol.* **161**:19–29.
- IANC, 1983. *Nomina Anatomica*. Williams and Wilkins, Baltimore.
- Ilinsky, I. A., and Kultas-Ilinsky, K. 1982. Stereotactic surgery in the rhesus monkey (*Macaca mulatta*) utilizing intracerebral landmarks. *Appl. Neurophysiol.* **45**:563–572.
- Koenig, J. F. R., and Klippel, R. A. 1963. *The Rat Brain: A Stereotaxic Atlas of the Forebrain and Lower Parts of the Brain Stem*. Williams and Wilkins, Baltimore.
- Krieg, W. J. S. 1975. *Interpretive Atlas of the Monkey's Brain*. Brain Books, Evanston, IL.
- Kusama, T., and Masako, M. 1970. *Stereotaxic Atlas of the Brain of Macaca fuscata*. Univ. Park Press, Baltimore.
- Martin, R. F., Dubach, J., and Bowden, D. M. 1990. NeuroNames: Human/maaque neuroanatomical nomenclature. In *Fourteenth Annual Symposium on Computer Applications in Medical Care: Standards in Medical Informatics*, Washington, DC (R. A. Miller, Ed.), pp. 1018–1019. IEEE Comput. Soc. Press, Los Alamitos, CA.
- Mazziotta, J. C., Toga, A. W., Evans, A., Fox, P., and Lancaster, J. 1995. A probabilistic atlas of the human brain: Theory and rationale for its development. *Neuroimage* **2**:89–101.
- Mesulam, M.-M., Mufson, E. J., Levey, A. I., and Wainer, B. H. 1983. Cholinergic innervation of cortex by the basal forebrain: Cytochemistry and cortical connections of the septal area, diagonal band nuclei, nucleus basalis (substantia innominata), and hypothalamus in the rhesus monkey. *J. Comp. Neurol.* **214**:170–197.
- Oertel, G. 1969. Zur Zyto- und Myeloarchitektonik des Rhombencephalon des Rhesusaffen (*Macaca mulatta* Zimmerman). *J. Hirnforsch.* **11**:377–405.
- Olszewski, J. 1952. *The Thalamus of the Macaca mulatta: An Atlas for Use with the Stereotaxic Instrument*. Karger, Basel.
- Paxinos, G. 1990. *The Human Nervous System*. Academic Press, Los Angeles.
- Paxinos, G., and Watson, C. 1986. *The Rat Brain in Stereotaxic Coordinates*. Academic Press, San Diego.
- Pellegrino, L. J., and Cushman, A. J. 1967. *A Stereotaxic Atlas of the Rat Brain*. Appleton-Century-Crofts, New York.
- Percheron, G. 1975. Ventricular landmarks for thalamic stereotaxy in *Macaca*. *J. Med. Primatol.* **4**:217–244.
- Percheron, G., and Lacourly, N. 1973. L'imprecision de la stereotaxie thalamique utilisant les coordonnees craniennes de Horsley-Clarke chez le macaque. *Exp. Brain Res.* **18**:355–373.
- Rebert, C. S., Hurd, R. E., Matteucci, M. J., De LaPaz, R., and Enzmann, D. R. 1991. A procedure for using proton magnetic resonance imaging to determine stereotaxic coordinates of the monkey's brain. *J. Neurosci. Methods* **39**:109–113.
- Riley, H. A. 1943. *An Atlas of the Basal Ganglia, Brain Stem and Spinal Cord (Based on Myelin-Stained Material)*. Williams and Wilkins, Baltimore.
- Sato, L., McClure, R. C., Rouse, R. L., Schatz, C. A., and Greenes, R. A. 1993. Enhancing the Metathesaurus with clinically relevant concepts: Anatomic representations. In *16th Annual Symposium on Computer Applications in Medical Care*, pp.388–391. McGraw-Hill, New York.
- Saunders, R. C., Aigner, T. G., and Frank, J. A. 1990. Magnetic resonance imaging of the rhesus monkey brain: Use for stereotactic neurosurgery. *Exp. Brain Res.* **81**:443–446.
- Schaltenbrand, G., and Wahren, W. 1977. *Atlas for Stereotaxy of the Human Brain*. Thieme, Chicago.
- Schiemann, T., Hoene, K. H., Koch, C., Pommert, A., Riemer, M., Schubert, R., and Tiede, U. 1994. Interpretation of tomographic images using automatic atlas lookup. In *Visualization in Biomed-*

- cal Computing* (R. A. Robb, Ed.), pp. 457–465. SPIE—Int. Soc. Opt. Eng., Bellingham, WA.
- Shantha, T. R., Manocha, S. L., and Bourne, G. H. 1968. *A Stereotaxic Atlas of the Java Monkey Brain (Macaca irus)*. Karger, Basel.
- Simmons, D. M. 1979. Egg yolk embedding for frozen sections of whole primate brain segments. *J. Histotechnol.* **2**:62–66.
- Smith, O. A., Kastella, K. G., and Randall, D. R. 1972. A stereotaxic atlas of the brainstem for *Macaca mulatta* in the sitting position. *J. Comp. Neurol.* **145**:1–24.
- Snider, R. S., and Lee, J. C. 1961. *A Stereotaxic Atlas of the Monkey Brain (Macaca mulatta)*. Univ. Chicago Press, Chicago.
- Stephan, H., Baron, G., and Schwerdtfeger, W. K. 1980. *The Brain of the Common Marmoset (Callithrix jacchus): A Stereotaxic Atlas*. Springer-Verlag, Berlin.
- Swanson, L. W. 1992. *Brain Maps: Structure of the Rat Brain*. Elsevier, Amsterdam.
- Szabo, J., and Cowan, W. M. 1984. A stereotaxic atlas of the brain of the cynomolgus monkey (*Macaca fascicularis*). *J. Comp. Neurol.* **222**:265–300.
- Talairach, J., David, M., Tournoux, P., et al. 1957. *Atlas D'Anatomie Stereotaxique*. Masson, Paris.
- Talairach, J., and Tournoux, P. 1988. *Co-planar Stereotaxic Atlas of the Human Brain*. Thieme, New York.
- Taylor, A. E. 1959. *Calculus with Analytic Geometry*. Prentice Hall, Englewood Cliffs, NJ.
- Toga, A. W. 1994. Visualization and warping of multimodality brain imagery. In *Functional Neuroimaging: Technical Foundations* (R. W. Thatcher, M. Hallett, T. Zeffiro, E. R. John, and M. Huerta, Eds.), pp. 171–180. Academic Press, San Diego.
- Turner, B. H., Gupta, K. C., and Mishkin, M. 1978. The locus and cytoarchitecture of the projection areas of the olfactory bulb in *Macaca mulatta*. *J. Comp. Neurol.* 381–396.
- Tuttle, M., Sheretz, D., Olson, N., Erlbaum, M., Sperzel, D., Fuller, L., and Nelson, S. 1990. Using Meta-1—The first version of the UMLS Metathesaurus. In *Fourteenth Annual Symposium on Computer Applications in Medical Care*, pp. 131–135. IEEE Computer Society Press, Los Alamitos, California.
- Ungerstedt, U. 1971. Stereotaxic mapping of monoamine pathways in the rat brain. *Acta Physiol. Scand.* **82**:1–48.
- Winters, W. D., Kado, R. T., and Adey, W. R. 1969. *A Stereotaxic Brain Atlas for Macaca nemestrina*. Univ. of California Press, Los Angeles.